Optimization of footbridges composed of prismatic tensegrity modules

ASCE Journal of Bridge Engineering

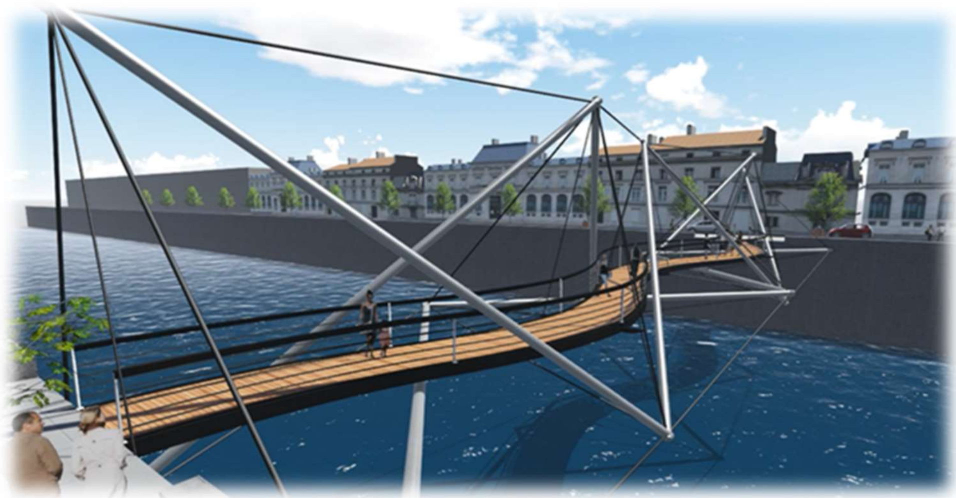

Jonas FERON, Lindy BOUCHER, Vincent DENOEL, Pierre LATTEUR

References of the article:

Feron Jonas, Boucher Lindy, Denoël Vincent, Latteur Pierre, 2019, “Optimization of footbridges composed of prismatic tensegrity modules”, **Journal of Bridge Engineering**; 24 (12): 04019112 p. 1-28

The last edition of this article is available online:

https://ascelibrary.org/doi/abs/10.1061/%28ASCE%29BE.1943-5592.0001438

Contact: pierre.latteur@ucouvain.be, jonas.feron@uclouvain.be

Thank you for your interest,
The authors

Optimization of footbridges composed of prismatic tensegrity modules

Jonas Feron[1,2], Lindy Boucher[1], Vincent Denöel[3], Pierre Latteur[1]

[1]Université catholique de Louvain, UCL,
Louvain School of Engineering EPL, Civil and Environmental Engineering,
Place du Levant, 1 (Vinci), bte L5.05.01, 1348-Louvain-la-Neuve, Belgium,
pierre.latteur@uclouvain.be

[2]BESIX,
Avenue des communautés, 100, 1200 Bruxelles, Belgium
jferon@besix.com

[3]Université de Liège, ULg,
Faculté des Sciences Appliquées, Argenco,
Quartier Polytech 1, Allée de la découverte, 9, 4000 Liège, Belgium,
v.denoel@ulg.ac.be

Abstract

The architectural potential of tensegrity structures is proven. Yet, paradoxically, very few real construction projects have been built around the world. The main reasons are complex construction processes, lack of design and optimization guidelines, and excessive self-weight due to the pre-stress needed to guarantee stiffness and dynamic behavior. Hence, optimizing the stiffness and self-weight is a key aspect when designing a tensegrity footbridge. Previous research by the same authors (Latteur et al., 2017) has demonstrated the validity of a design and optimization methodology that identifies, for a family of structures, geometry with a maximum stiffness or/and a minimum self-weight. In this article, that methodology is applied to footbridges composed of tensegrity modules comprising simplex, quadruplex, pentaplex and hexaplex. A comparison of the stiffest and lightest structures is provided, a practical case study is developed, and the relevance and feasibility of such tensegrity footbridges discussed. As a result, the study provides advice on optimum footbridge topologies with the following characteristics: excellent stiffness and dynamic behavior; efficient structures composed of simplex modulus; the self-weight is still rather high, but similar to bended structures, although with potential to reduce with the optimization of the pre-stress scenario.

Keywords: tensegrity, footbridge, optimization, feasibility, stiffness, volume, mass, self-weight, morphological indicators, simplex, quadruplex, pentaplex, hexaplex

1. State of the art and objectives

Tensegrity is a word with controversial definitions (Hanaor, 2012). A tensegrity system often refers to a system in a stable self-equilibrated state comprising a discontinuous set of compressed components inside a continuum of tensioned components (Motro, 2005). In order to widen the potential of tensegrity to engineering applications, it is also often considered that a tensegrity structure may have k compressive components in contact on a same node. In this case one talks about a structure “of class k”. Other definitions can include “extended tensegrity structures” with some members subjected to bending moments, structures which are pre-stressable if only supports exist, etc.

Although tensegrity and extended tensegrity structures have found a large place into scientific papers these last decades, the topic of tensegrity applied to footbridges is relatively absent into the literature. In his book published in 2010 (Jáuregui), 2010, Jáuregui establishes a large state of the art about tensegrity structures and their application to architecture. He cites some authors suggesting the use of tensegrity for bridge applications, but his investigations do not reveal any existence of tensegrity based bridge proposals before 2004. He also cites some authors describing structures having, according to them, a high stiffness and economical design. Other cited authors, on the contrary, are more skeptical about their performances in comparison with more classical structures. Yet, nowadays, there is still a lack of rigorous and quantitative proofs about the structural efficiency or inefficiency of tensegrity structures for engineering applications, in particular bridges and footbridges.

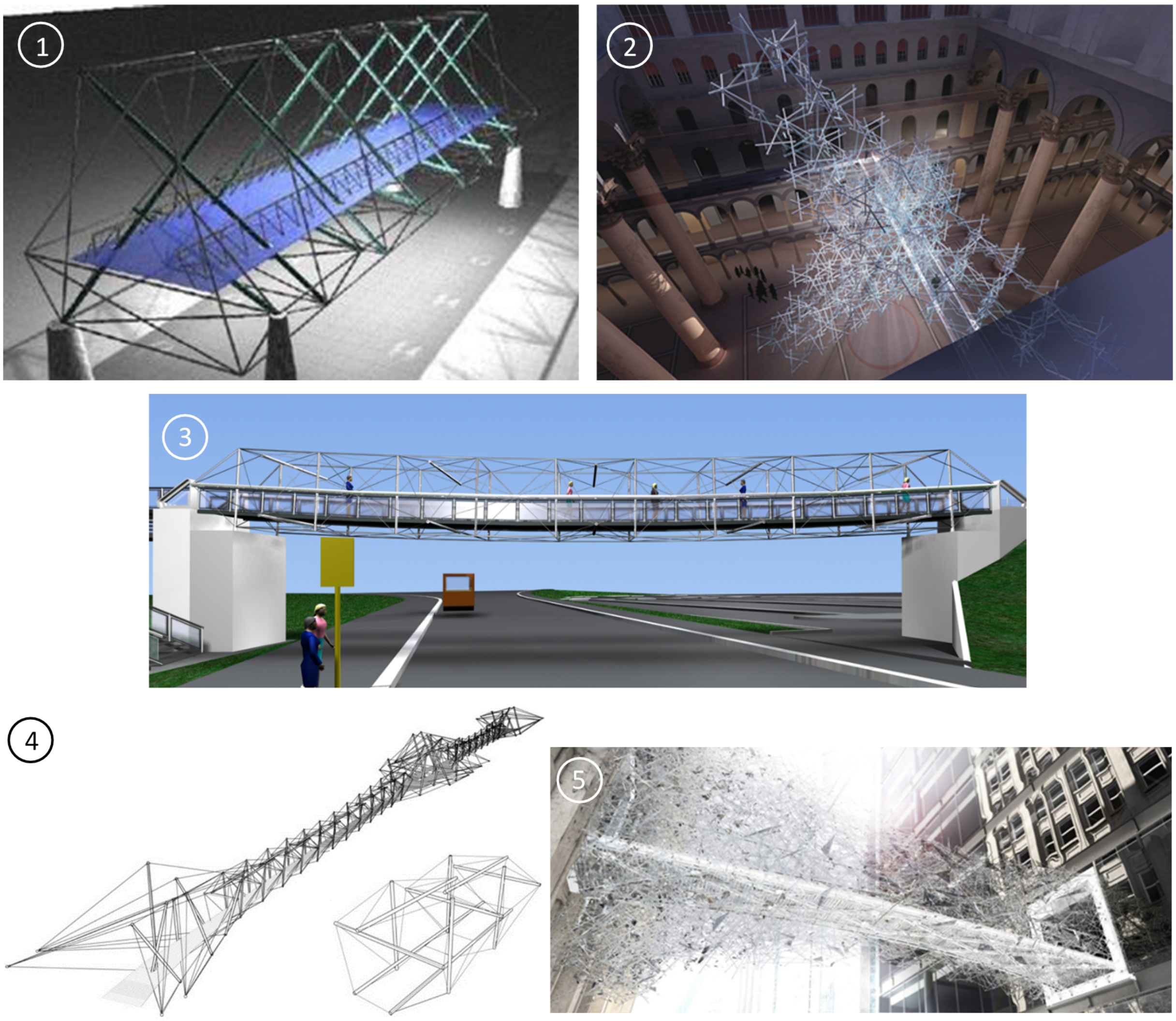

Fig. 1. Architectural projects: 1 - prototype of Jáuregui (Jáuregui, 2010), 2 - prototype of WilkinsonEyre (WilkinsonEyre, 2004, reprinted with permission), 3 - Tor Vergata footbridge (Micheletti et al., 2005, reprinted with permission), 4 - Suspended tensegrity bridge (Mucedola and Paradiso, 2013), 5 - Splash bridge (Grozdanic, 2011).

Figure 1 shows a few creative prototypes with a high architectural potential, which however never reached the construction stage:

- In his end master thesis, Jáuregui proposes a class 1 (no struts in contact with each other) tensegrity footbridge concept based on a succession of simplex modules (figure 1-1);
- In 2004, the architects WilkinsonEyre with the structural engineer C. Balmond from Arup develop a prototype of a 35m long tensegrity bridge composed of a mesh of tetrahedral cells (figure 1-2). The footbridge was designed in order to span across the Great Hall of the National Building Museum in Washington D.C. and to react to pedestrians by lighting the glass struts subjected to changing stresses (Davey and Forster, 2007);
- In 2005, Micheletti et al. present the Tor Vergata footbridge (figure 1-3), a 32m long tensegrity footbridge of class 2 which is composed of “re-expanded octahedron” modules. The height

(3.6m), the number of modules (5), the sections of the struts (193mm of diameter, 12mm thick) and of the cables (72mm) are chosen in order to find a compromise between maximum stiffness (deflection of 8cm under the most critical static loads combination) and cost efficiency (Micheletti, 2012);

- In 2010, Mucedola and Paradiso propose the suspended tensegrity bridge project (figure 1-4) which aims at crossing the Sesia river (Italy) for the sake of the 5900km bicycle route of the European facilities program “EuroVelo 8”. The extended tensegrity footbridge, based on a reviewed “re-expanded octahedron” module, consists in two main spans of 117m and 78m, with a height of 7m (headroom of 2.85m) and a straight 3.1m wide deck. The struts have a diameter of 300 mm with a thickness of 10mm, while the cables have a diameter of 40mm (Mucedola and Paradiso, 2013);
- In the “Building to building pedestrian bridge” challenge proposed by the internet community “Designbymany” in 2011, Cullum proposed his “Splash” bridge design (figure 1-5) (Grozdanic, 2011). Here, the tensegrity is actually not the main footbridge structure but a secondary structure that surrounds it.

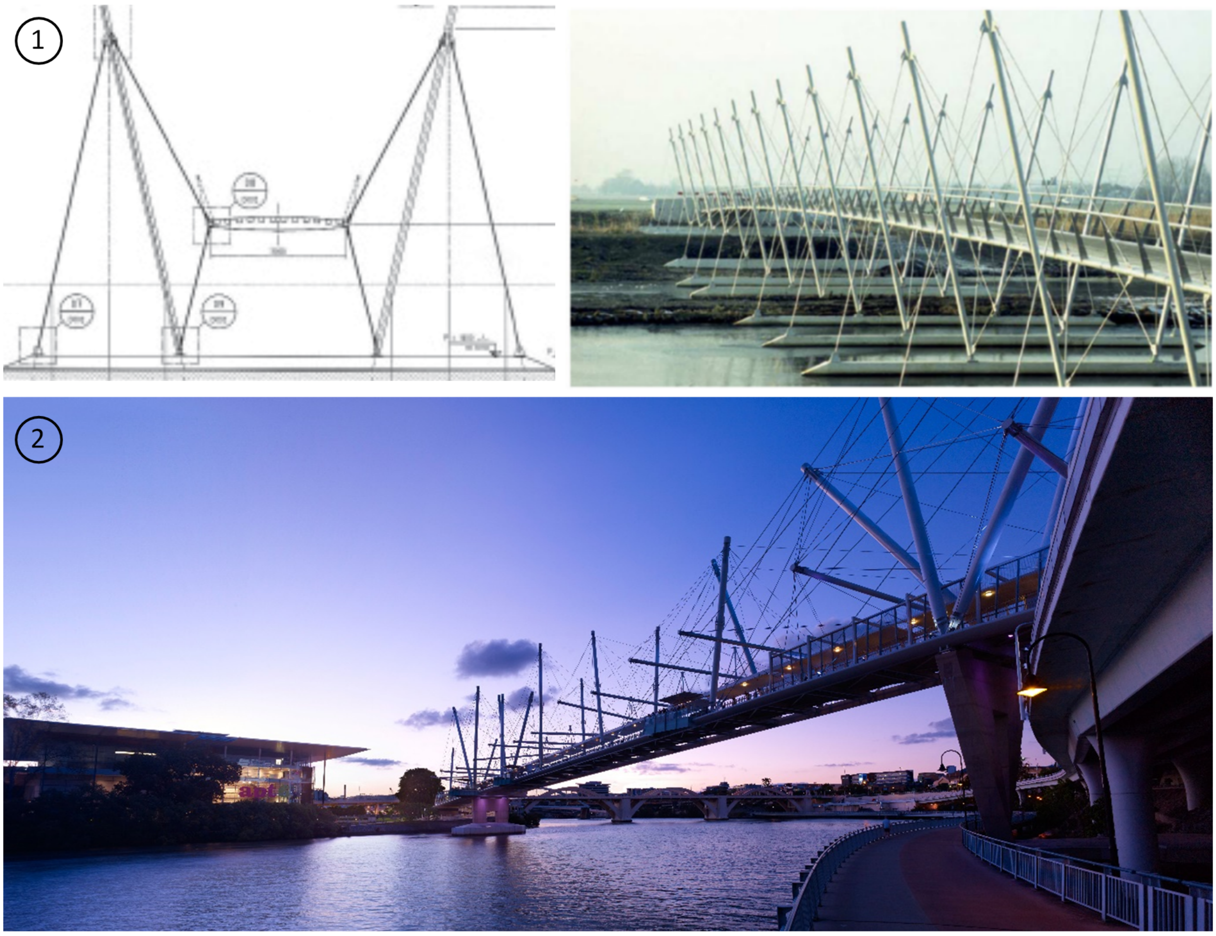

Fig. 2. Existing footbridges: 1 - Bridge of Masts (2000, Purmerend, Netherlands) by den Hollander (Eekhout, 2016, reprinted with permission), 2 - Kurilpa Bridge (2009, Brisbane, Australia) by Cox Rayner Architects and Arup.

Nevertheless, figure 2 shows 2 rare examples of existing footbridges based on the tensegrity principle:

- In 2000, the architect den Hollander (Eekhout, 2016) designed the *Bridge of Masts* in Purmerend (Netherlands), based on extended tensegrity. This 144m long pedestrian bridge is supported by two rows of 16 masts and 64 tensile rods in such way that the 3.5m wide deck is suspended and visually independent of the masts (figure 2-1);

- In 2009, Cox Rayner Architects and Arup designed the Kurilpa Bridge (Brisbane, Australia). In 2010, Rolvink et al. from Arup describe this 470m long (main span of 120m) pedestrian bridge as a multi-mast cable-stay structure, inspired by the principle of tensegrity (figure 2-2), which is “both lightweight and incredibly strong”.

Finding the feasibility range of tensegrity (foot)bridges on the basis of structural performances as stiffness or self-weight remains a complex problem due to the non-linear calculation combined with the large number of parameters that characterize such structures: the pre-stress, the topology, the span, the width, the height, the characteristics of the cross-sections, the characteristics of the materials, the external loads, etc.

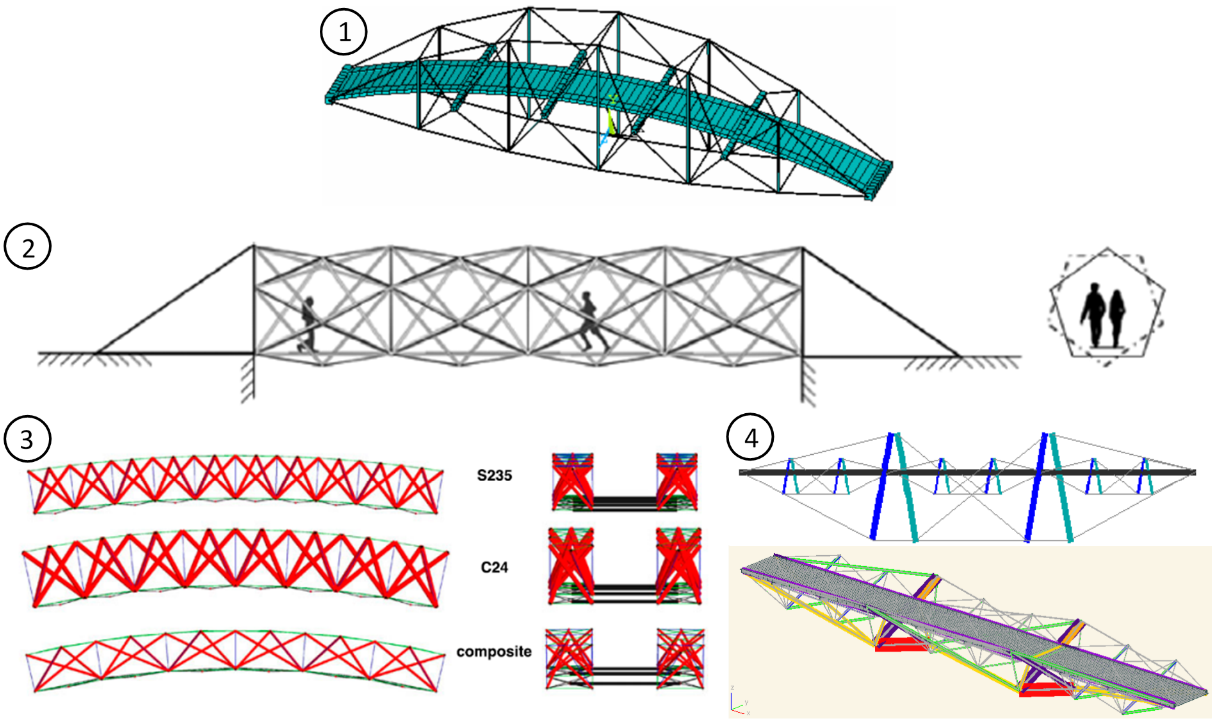

Fig. 3. Optimized bridge projects using tensegrity principle: 1 - Tensegrity bridge with a prestressed deck (Briseghella et al., 2010), 2 - Hollow-rope footbridge (2006) (Barbarigos, Bel Hadj Ali et al. 2010, reprinted with permission) , 3 - curved tensegrity beams (Amouri et al., 2014, reprinted with permission), 4 - prototype (De Boeck, 2013).

Figure 3 shows different bridge designs using the tensegrity principle, which have been calculated/optimized according to different methodologies:

- In 2010, Briseghella et al. study the influence of the height of the structure, of the prestress and of the dimensions of the slab, beams and cables on the dynamic behavior of a 30m long footbridge (figure 3-1). The pre-stressed arch deck is supported by four transverse rectangular beams (500x200x10mm) which, together, are part of the extended tensegrity system. The pre-tensioned steel struts (25mm, 1000MPa) provide the stiffness;
- From 2010 on, several authors bring a significant contribution in the design of footbridges composed of tensegrity modules. They study the influence of several parameters on the structural behavior (Rhode-Barbarigos, Jain, et al., 2010 and Rhode-Barbarigos, Bel Hadj Ali, et al., 2010), analyze the dynamical behavior (Bel Hadj Ali et al., 2010), control numerically and experimentally the deployment (Rhode-Barbarigos et al., 2012 and Veuve et al., 2015 and Sychterz and Smith, 2017), present a feasible configuration of a 20m span class 2 tensegrity pedestrian bridge initially proposed by Motro et al. in 2006 (figure 3-2). In particular, (Rhode-Barbarigos, Bel Hadj Ali, et al., 2010) describe a design/optimization process based on

parametric analysis of the cross-sectional area of the struts and cables, of the rigidity ratio (cables/struts) and of the self-stress level. Their method allows to compare different modules topologies (square, pentagonal, hexagonal) thanks to a "Structural Efficiency Index" which takes into account both the self-weight and the deflection of the structure;

- In 2012, Averseng and Dubé compare the performances, in terms of mass and deflection, of different geometries of a class 2 deployable 12m tensegrity beam composed of a succession of quadruplex modules. Their optimization methodology consists in progressively increasing the pre-stress level and cross-sectional area until both no slacked cable criterion and allowable stresses are respected. The optimal tensegrity beam minimizing their "performances indicator" (defined as the inverse of the product of the deflection and the mass) shows high deflection (L/130) and important mass compared to traditional beams. In 2014, Amouri et al. improve their algorithm and present 3 curved tensegrity beams with 3 different geometries and various materials (figure 3-3).
- In 2013, De Boeck presents an extended tensegrity topology based on a succession of simplex modules according to a fractal design (figure 3-4). In each simplex module, one strut is horizontal and supports the deck. He details such a 30m span structure weighing 270kN, able to support a distributed load of 6.25kN/m with a maximum deflection of 55mm;
- In 2014 and 2015, according to the extended definition of tensegrity (Skelton and Oliveira, 2009), Skelton, Carpentieri et al. find the minimum mass design of a simply supported 2D tensegrity bridge carrying distributed loads. The fractal principle is used through a repetition of the minimal mass module of Michell (Michell, 1904). Their methodology consists in finding the analytical expression of a dimensionless mass indicator in function of the topology and to minimize it under material yielding or buckling constrain.

Finally, in 2017, Latteur et al. present a design methodology based on a stiffness and volume/mass optimization algorithm for 3D nonlinear hyperstatic and pre-stressed structures composed of elements only subjected to axial forces, with a special emphasis on tensegrity structures. The methodology is based on dimensionless numbers called morphological indicators that allow reducing the amount of parameters to consider for the stiffness and mass optimization process. It allows to rigorously find the best topologies within a given family of structures (the best ratio L/H, the best number of tensegrity modules). The article first demonstrates the optimization algorithm and then gives numerical confirmations and examples. In particular, Latteur et al. propose, as an illustration of their design methodology, a geometry of tensegrity footbridge composed of a succession of elementary tensegrity simplex, called "the snake bridge" (figure 4). The sinusoidal design of the deck comes naturally from the fact that it significantly increases the architectural value, but also the headroom for pedestrians, since the upper nodes of the structures are not aligned.

This paper mainly focuses on the topic related to tensegrity footbridges themselves. Concerning the morphological indicators and the other design methodologies for tensegrity structures, a detailed state of the art can be found in (Latteur et al, 2017).

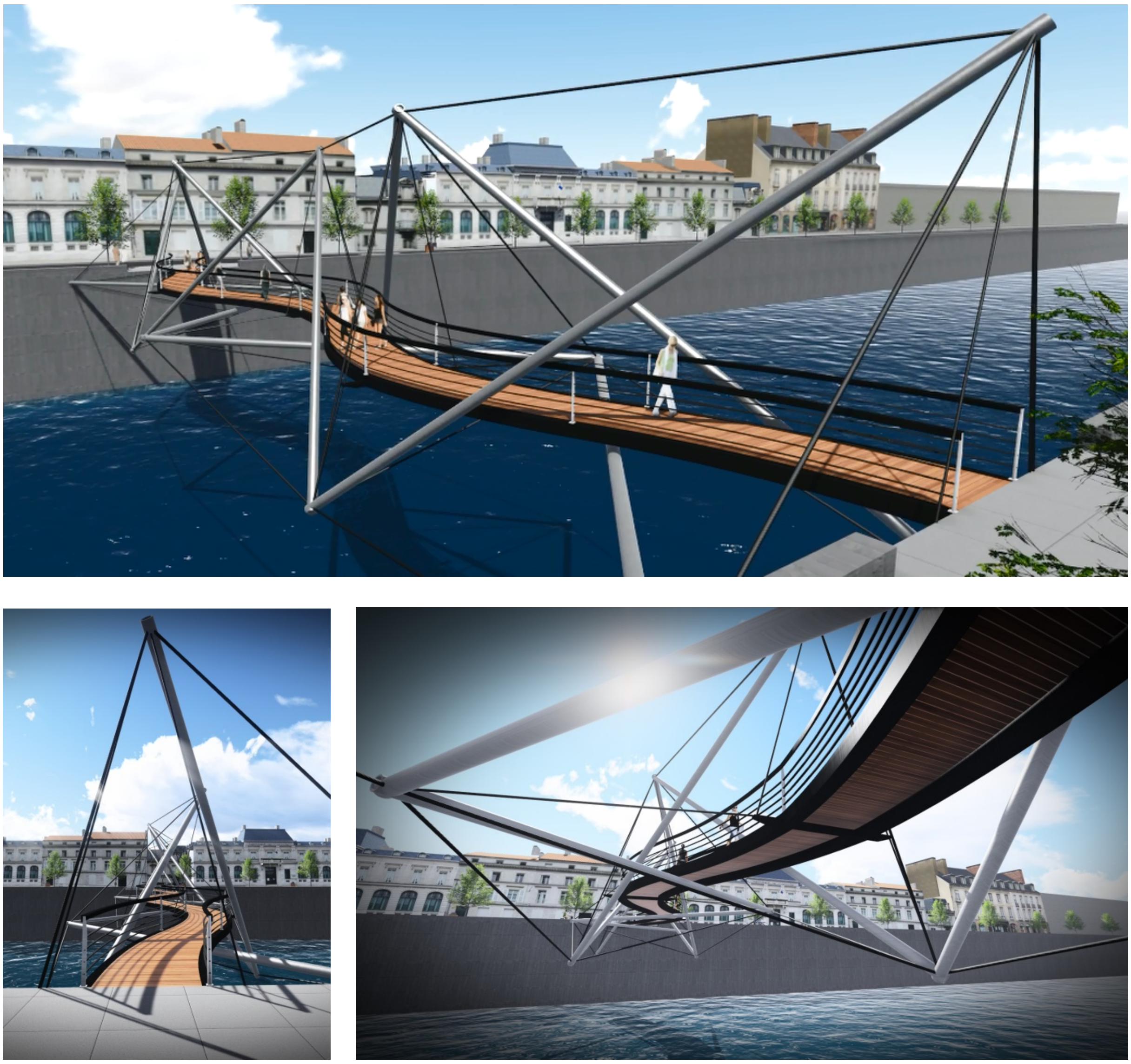

Fig. 4. The “snake footbridge”, a design proposed by Latteur et al. in 2017.

The aim of this article is to develop and use the design methodology demonstrated in (Latteur et al, 2017) in order to prove the feasibility of footbridges composed of a succession of elementary tensegrity modules of type simplex, quadruplex, hexaplex and pentaplex (figures 4, 5, 7 and 10), with a suspended deck situated inside the main class 2 tensegrity structure. In other words, the study aims at selecting the types of tensegrity module, their number “*S*”, and the ratios *L/H* (span over height) that lead to the lightest and/or stiffest structures. The relevance of this type of construction with respect to other types of structures such as trusses is discussed and a practical example of a 40m long footbridge is given.

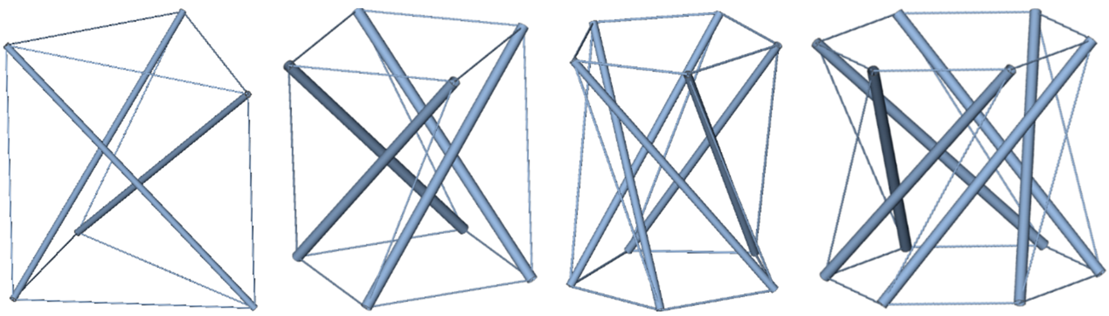

Fig. 5. From left to right, the simplex, the quadruplex, the pentaplex and the hexaplex.

2. Assumptions and definitions

2.1. General assumptions

This article considers any structure:

- Of span *L*, height *H* and width *D*, considered after application of the pre-stress (figure 7) and composed of a number *S* of elementary tensegrity modules of type simplex, quadruplex, pentaplex or hexaplex (figure 5);
- With n_c cables made out of the same material of specific weight ρ_c, Young modulus E_c, and design strength σ_c;
- With n_s struts made out of the same material of specific weight ρ_s, Young modulus E_s and design strength σ_s, and such that factor *u* is defined as $u=\sigma_c/\sigma_s$;
- With materials having an elastic linear behavior, σ_c and σ_s coming respectively from the division of the characteristic yield strength by the adequate security coefficient (this is discussed in the next section);
- With struts having cross sectional areas A_s and moments of inertia I_s, such that the form factor *q*, defined as $q = I_s / A_s^2$ (Figure 6), is supposed to be equal for all struts;

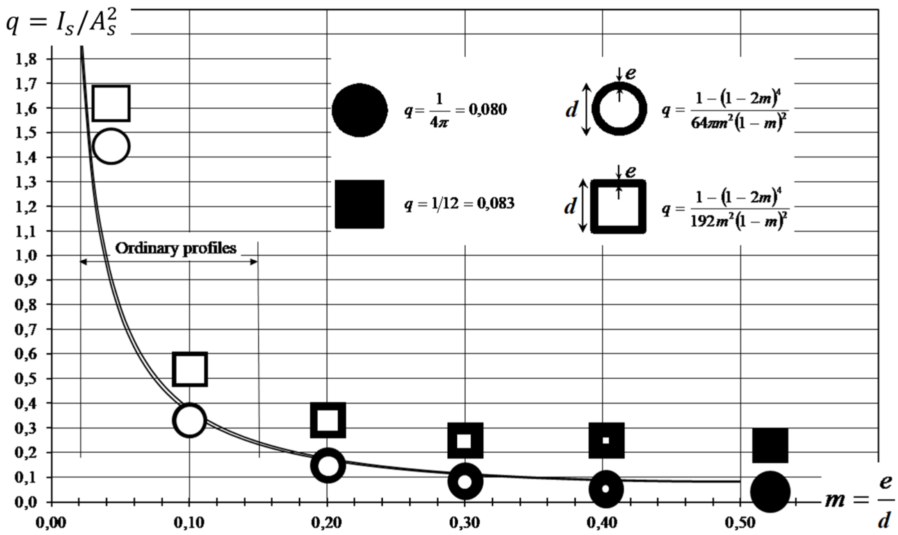

Fig. 6. Values of the form factor $q = I_s / A_s^2$ for usual cross sections.

- In which each cable (or any element remaining always in tension) of index *i*, subjected to a tension force $N_{c,i}$, has a cross sectional area $A_{c,i}$ related to the design criterion: $N_{c,i} / A_{c,i} = \sigma_c$ (1a)
- In which each strut of index *i* and length $L_{0,i}$, subjected to a compression force $N_{s,i}$, has a cross sectional area $A_{s,i}$ related to the design criterion (approximation of corrected Euler's law):

$$\frac{N_{s,i}}{A_{s,i}} = \frac{1}{1+\Lambda_i^2}\sigma_s \qquad \text{with} \qquad \begin{cases} \Lambda_i = \lambda_i \Big/ \left(\pi\sqrt{E_s/\sigma_s}\right) \\ \lambda_i = L_{0,i}\sqrt{A_{s,i}/I_{s,i}} \end{cases} \quad \text{(1b)}$$

- In which cables and struts are designed according to 1a and 1b and, although the methodology allows a fully stressed design, in this article:
    - All struts have the same cross-sectional area A_s (and diameter d_s), provided by the most stressed strut;
    - Longitudinal cables have the same cross-sectional area $A_{c,l}$ (and diameter $d_{c,l}$) and transversal cables have the same cross-sectional area $A_{c,t}$ (and diameter $d_{c,t}$). This

assumption comes from the observation that the longitudinal cables are usually more stressed than the transversal ones.

- With a maximum deflection δ somewhere, for instance at mid-span and vertically, considering that δ is created both by the external load $\tilde{\mathbf{F}}$ and self-weight $\tilde{\mathbf{G}}$;
- Related to an indicator of buckling Ψ developed by (Latteur, 2000) and such that: $\Psi = \sigma_s L \big/ \sqrt{q E_s F}$;
- With a total volume V of materials (cables and struts).

2.2. External loads, self-weight, pre-stress and security coefficients

The usual structural design methodology consists in calculating the cross sections according to ULS combinations, and limiting the deflections according to the SLS combinations. Both depend on multiplication factors defined in the codes, which are not the same from one country to another and which have particular values for dead loads, live loads, wind, snow, etc. The ratio between ULS and SLS combinations usually varies between 1,35 and 1,5. This way of designing must also take into account a security about both the accidental loss of pre-stress and the accidental excessive pre-stress, as well as security coefficients on the characteristic yield strengths of materials (that usually vary from 1 to 1.5, depending on the material). Globally, such ULS/SLS design is uneasy to associate with an optimization methodology. Indeed, the assumptions about the multiplication factors related to ULS and SLS combinations, the range of security to consider for the pre-stress, and the security coefficients to consider for the materials pollute the analysis and the objective comparison between the different topologies. This is the reason why, in this article, ULS and SLS combinations are not considered: live load $\tilde{\mathbf{F}}$ and self-weight $\tilde{\mathbf{G}}$ are not multiplied with any multiplication factor. However, a way to consider all those uncertainties is to include them into a single global security coefficient applied on the materials only. In particular for the results given in this article, steel with a characteristic yield strength of 355MPa is considered, associated with a global security coefficient of 1,5 , that means :

- A design strength equal to $\sigma=\sigma_c=\sigma_s$=355/1.5=237MPa;
- An Elastic modulus equal to $E=E_c=E_s$=210000MPa;
- Ratios $E/\sigma=E_c/\sigma_c=E_s/\sigma_s$=886;
- A volumic weight $\rho=\rho_c=\rho_s$=77 kN/m^3.

The combination of the external load cases acting in the 3 directions (X,Y,Z) on the n nodes of the structure is given by vector $\tilde{\mathbf{F}}$, such as:

$$\tilde{\mathbf{F}} = F\tilde{\mathbf{f}} = F\left(t_1^F, t_2^F, \ldots, t_i^F, \ldots, t_{3n}^F\right),$$

Where: $\begin{cases} \tilde{\mathbf{f}} = \left(t_1^F, t_2^F, \ldots, t_i^F, \ldots, t_{3n}^F\right) \\ -1 \le t_i^F \le 1 \\ \sum \left|t_i^F\right| = 1 \end{cases}$

Values of Ft_i^F are specified in figure 10 for each topology.

Self-weight is taken into account by assuming that each strut or cable connected to a node adds to this node a vertical load equal to the half of its own self-weight. Self-weight is thus considered as a new “external” load case $\tilde{\mathbf{G}}$ added to $\tilde{\mathbf{F}}$, $\tilde{\mathbf{G}}$ being a $3n$ dimension vector where only the components related to the vertical axis are non-null.

A judicious choice of pre-stress scenario $\tilde{\mathbf{P}}$ is necessary, to ensure the stability of the structure, to prevent some cables from slack when the external load case $\tilde{\mathbf{F}}$ and self-weight $\tilde{\mathbf{G}}$ are considered and, finally, to reach the desired stiffness.

Vector $\tilde{\mathbf{P}}$ is composed of the n_c+n_s values of the axial force P_i in each element, cable or strut (with tension for cables and compression for struts). Those values are thus the internal axial forces that exist *before* the application of the external load $\tilde{\mathbf{F}}$ and self-weight $\tilde{\mathbf{G}}$. The pre-stress scenario $\tilde{\mathbf{P}}$ is defined as followed:

$$\tilde{\mathbf{P}}=\beta F\tilde{\mathbf{p}}=\beta F\left(t_1^p,t_2^p,\ldots,t_i^p,\ldots,t_{n_c+n_s}^p\right),\text{ where: }\begin{cases}\tilde{\mathbf{p}}=\left(t_1^p,t_2^p,\ldots,t_i^p,\ldots,t_{n_c+n_s}^p\right)\\ \quad\text{is the pre-stress state}\\ -1\le t_i^p\le 1\\ \beta\ge 0\text{ is the pre-stress level}\end{cases}$$

A self-stress mode is a particular value of $\tilde{\mathbf{p}}$ which maintains the initial geometry of the structure, while a self-stress state is either a self-stress mode either the combination of several self-stress modes.

For a pre-stress state $\tilde{\mathbf{p}}$ judiciously chosen, β_{min} is defined as being the particular value of β that leads to a situation where the axial force into the least tensioned cable after consideration of the external load $\tilde{\mathbf{F}}$ and self-weight $\tilde{\mathbf{G}}$ is equal to zero, which means that no cable slacks:

$\beta=\theta\beta_{min}$, with $\theta\geq 1$.

In this paper, $\theta=1$ and $\beta=\beta_{min}$ will be assumed and the way to find the value β_{min} is discussed in (Latteur, 2017). The impact of $\theta<1$ or $\theta>1$ is discussed in the conclusion of this article.

As detailed in (Latteur et al, 2017), a way to numerically create a pre-stress scenario $\tilde{\mathbf{P}}$ is to numerically apply to each element of the structure an external axial force $\tilde{\mathbf{F}}_{\mathbf{pre},i}$ at its extremities. This leads, after calculation, to a situation where each element of the structure, including the ones in which $\tilde{\mathbf{F}}_{\mathbf{pre},i}$ was initially introduced as external load, is finally subjected to a force P_i different from $\tilde{\mathbf{F}}_{\mathbf{pre},i}$.

The (n_c+n_s) values of the initial axial force $\tilde{\mathbf{F}}_{\mathbf{pre},i}$ can be defined by vector $\tilde{\mathbf{F}}_{\mathbf{pre}}$:

$$\tilde{\mathbf{F}}_{\mathbf{pre}}=\beta_{pre}F\tilde{\mathbf{f}}_{\mathbf{pre}}=\beta_{pre}F\left(t_1^{pre},t_2^{pre},\ldots,t_i^{pre},\ldots,t_{n_c+n_s}^{pre}\right),\text{ with: }\begin{cases}\tilde{\mathbf{f}}_{\mathbf{pre}}=\left(t_1^{pre},t_2^{pre},\ldots,t_i^{pre},\ldots,t_{n_c+n_s}^{pre}\right)\\ -1\le t_i^{pre}\le 1\\ \beta_{pre}\ge 0\end{cases}$$

$\beta_{pre,min}$, just like β_{min}, is defined as being the particular value of β_{pre} that leads to a situation where the axial force in the least tensioned cable after application of the external load $\tilde{\mathbf{F}}$ and self-weight $\tilde{\mathbf{G}}$ is equal to zero, which means that no cable slacks.

The proposed design methodology considers that the choice of $\tilde{\mathbf{f}}_{\mathbf{pre}}$ is arbitrary, chosen once for all. Note that there may exist a better choice of $\tilde{\mathbf{f}}_{\mathbf{pre}}$, which leads to a stiffer or lighter structure. In this article, one assumes that the values of $\tilde{\mathbf{f}}_{\mathbf{pre}}$ are null for the cables and identical for the struts: $\tilde{\mathbf{f}}_{\mathbf{pre}} = (0,\ldots,0,-1,\ldots,-1)$. This hypothesis corresponds to a practical situation where only struts are equipped with a mechanical device that can elongate them.

2.3. Supports, topologies, load cases and headroom

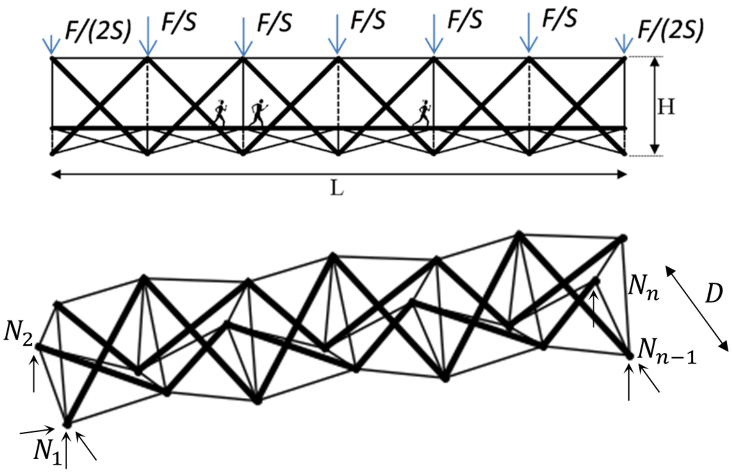

Fig. 7. Footbridge composed of a number *S* of elementary tensegrity simplex modules and subjected to a total external load *F* distributed on the upper nodes. The distribution of *F* depends on the topology (see details in figure 10).

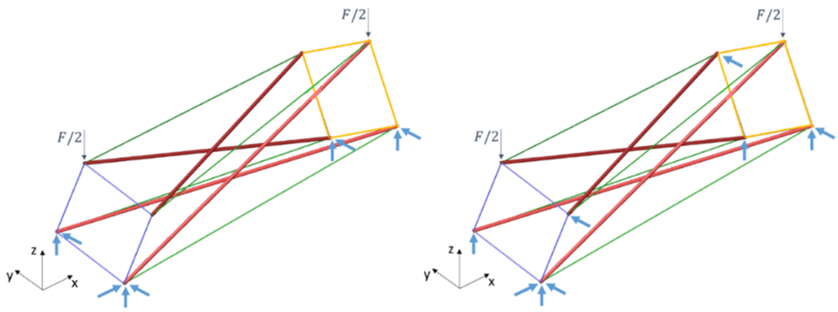

Fig. 8. For the same degree of redundancy, the position of the supports (shown by the small arrows) influences a lot the structural behavior. From this point of view, the situation on the right is much better than the situation on the left.

If R_s is the number of reactions at supports, the degree of redundancy D_r of such structures composed of *n* nodes is given by the following equation:

$$D_r = (n_c + n_s) + R_s - 3n$$

For each topology, many different positions of the supports can be chosen. For instance, the support on node N_2 is not essential to ensure the global stability of the structure shown in figure 7. However, support in N_2 improves a lot the structural behavior in terms of stiffness (in this case: D_r=(39+18)+7-3*21=1).

In order to perform a relevant comparison of the structures made out of different topologies (simplex, quadruplex, etc), a same degree of redundancy D_r equal to 1 is arbitrary chosen in this article.

Again, for a same degree of redundancy, several positions of the supports can be chosen, but some of them are not adequate. Figure 8 shows the simplified situation of a unique quadruplex where both situations correspond to D_r=1 and where the prestress is introduced via an identical elongation of the 4 struts. The structure on the left has very large displacements of the upper nodes when the external load $\tilde{\mathbf{F}}$ is applied, while the structure on the right has much more limited displacements. This example shows that the best choice of the position of the supports remains uneasy to formalize.

This article studies and compares 7 different topologies associated to their particular support positions and load distribution, as shown in figure 10. Concerning the distribution of the external load $\tilde{\mathbf{F}}$, it is assumed that each external force acts vertically on the upper nodes. Practically, this could be different, since the deck can be suspended to the upper nodes with more than one only cable, giving to the resultant of the force a horizontal component. The deck could also be supported by the below and/or the lateral nodes, which is not considered in this study.

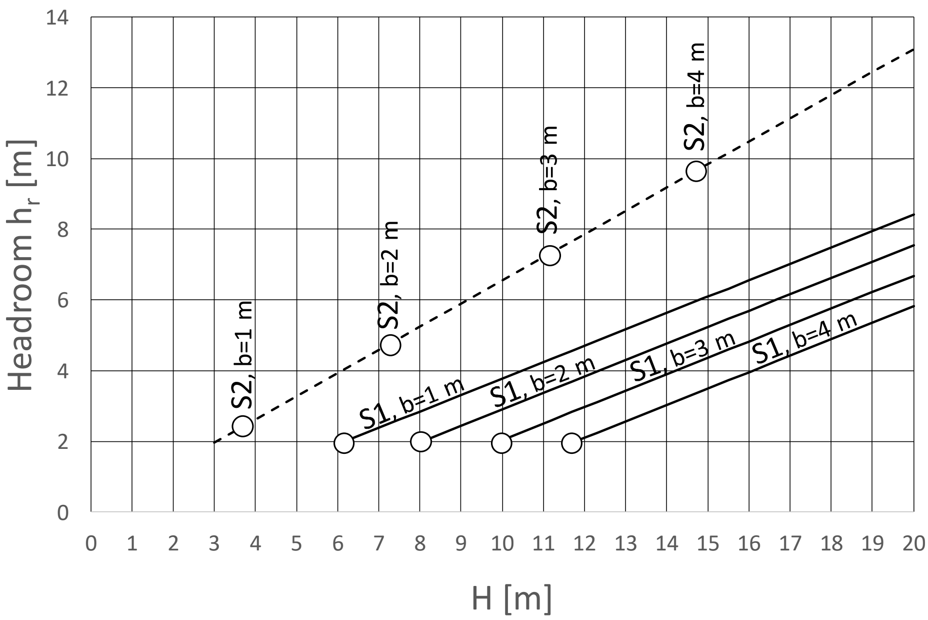

Fig. 9. Headroom inside a simplex for a straight deck configuration (S1) and for a snake deck configuration (S2).

An important topic is that the structures that do not allow a sufficient deck width b and headroom h_r should be omitted from the results of the optimization process. Figure 10 gives the formulas to evaluate the headroom for each topology. In this article, a minimum width b=2m and a minimum headroom h_r=2m will be considered in sections "General comparison of the 7 topologies" and "Practical example: 40 m span tensegrity footbridge". A value h_r=2m is indeed an absolute minimum value under which the construction of a footbridge would be irrelevant (in houses, many door openings have a 2m height).

A solution to increase the headroom for topology S1 is to change the straight geometry of the deck into a sinusoidal one (S1 then becomes the S2 topology), as shown in figure 4.

Figure 9 shows that:

- For S1 and S2, sufficient headroom (>2m) and deck width (>2m) need a height H of the structure, respectively, above 8m and 7m (Note however that other topologies as Q1 may offer better results in terms of h_r and b and may allow to reduce H until values around 5m, although these topologies are not efficient as shown further);
- For structures with a slenderness L/H between 3 and 7, which is the range where one finds the optimum structures as shown in tables 1 and 2, considering such structures for spans lower than 20 m has no sense, since the deck width and/or the headroom is insufficient.

2.4. Dynamic behavior

Footbridges are sensitive to pedestrian loading and the accelerations and deformation amplitudes that they experience must be limited. Although vibration criteria are implicitly covered in serviceability limit states (SLS), some codes suggest, especially in a pre-design stage, to keep the natural frequencies of the footbridge outside a critical frequency band. For instance, the Eurocode (NBN EN 1990/A1) suggests to avoid the ranges [0-2,5] Hz and [0-5] Hz, respectively for horizontal and vertical vibrations. Other design guidelines such as the Sétra (Setra, 2006), HiVoSS (Heynemeyer et al, 2009) or Tricon (Van den Broeck P. et al., 2012) give more precise information and are, therefore, usually preferred. For instance, the Setra guide recommends natural frequencies associated with horizontal vibrations outside the range [0.5-1.1] Hz and those associated with vertical vibrations outside the range [1.7-2.1] Hz, as well as its first few integer multiples. At the end of this paper (see section "Practical example: 40m span tensegrity footbridge"), a modal analysis of a S2 tensegrity footbridge is reported and indicates that it features natural frequencies outside the critical ranges. For this reason, the dynamic behavior criterion is not included in the discussion on optimality of this paper.

2.5. Allowable deflections

The limitation of the deflection is necessary for several reasons: behavior of supports, evacuation of water, aesthetic of the structure, vibrations and comfort of the pedestrians.

Concerning the live loads only, the deflection is often limited to values between *L*/250 and *L*/750, depending on the standards, or even from one project to another. For instance, §5 of 2009/2015 AASHTO's Guide Specifications for Design of Pedestrian Bridges (American Association of State Highway and Transportation Officials), states that "The deflection of the bridge due to the unfactored pedestrian live loading shall not exceed 1/360 of the span length".

Concerning the deflection δ due to dead loads combined with live loads, it is linked to the fundamental frequency "υ" of a footbridge and can be approximated with the following equation: $2\pi\upsilon[Hz] \cong \sqrt{9,81[m/s^2]/\delta[m]}$. This equation shows that, for a minimum fundamental frequency equal to 2.5Hz, δ should be limited to 0.04m, which means *L*/500, for a span of 20m. If the span or the required minimum fundamental frequency are higher, the stiffness criteria should be even stricter. Consequently, for large spans, the limitation of the deflection may be too restrictive to guarantee a minimum comfort to the pedestrians, and the vibration problem must then be solved by use of viscous or tuned mass dampers. Whatever the span, it is thus largely accepted that, the stiffer the structure is, the better it is.

In this article, a footbridge with a deflection under both live loads and self-weight greater than L/500 is considered being inefficient. This is of course an arbitrary choice, but globally in accordance with the above comments.

However, this study shows that the best structures in term of self-weight (essentially the structures composed of simplex modulus) have a surprisingly good stiffness, generally with a deflection lower than *L*/500. The removal of the few cases with δ/L>500 in section "General comparison of the 7 topologies" does not change the global results and conclusions of the article.

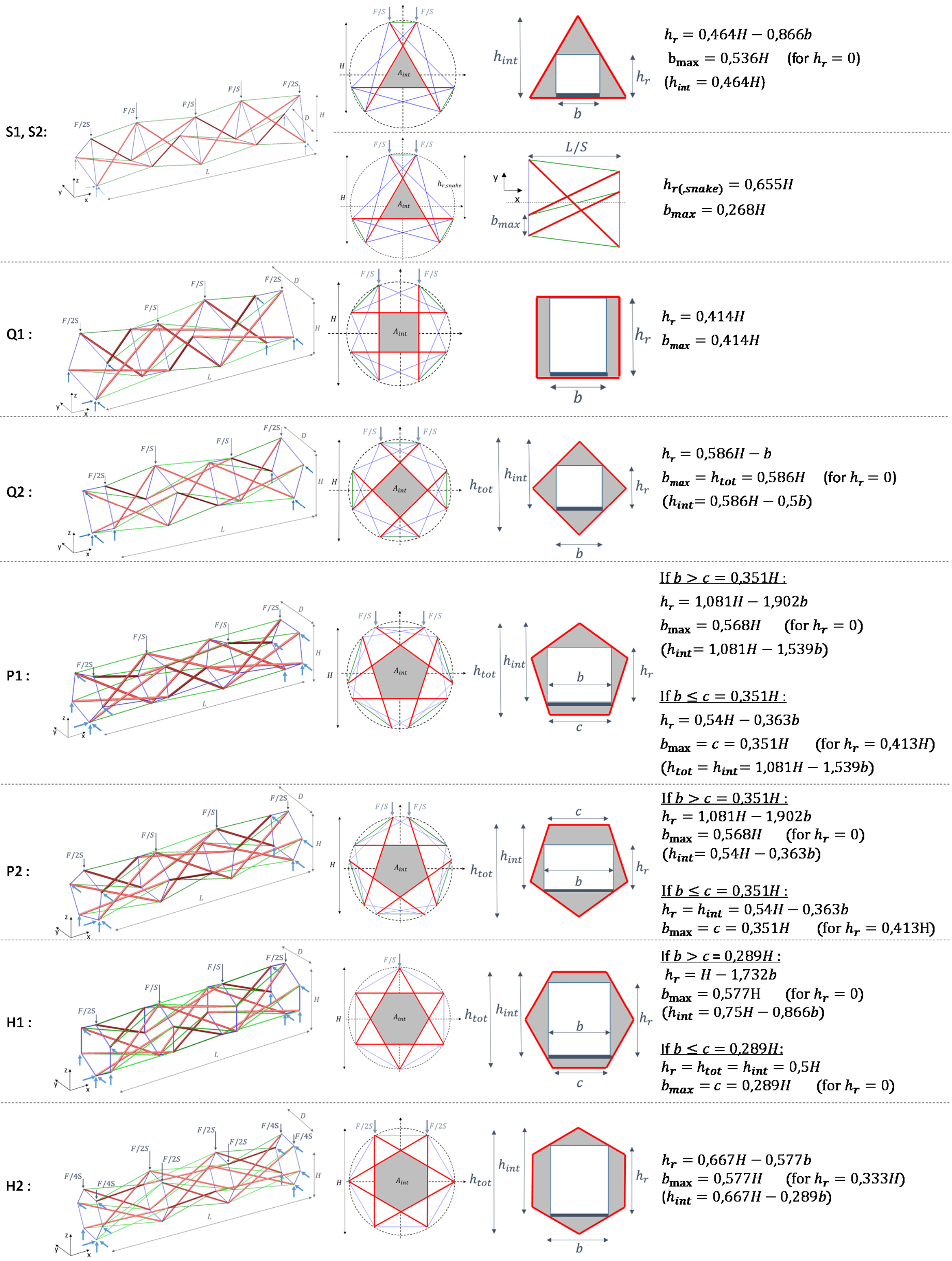

Fig. 10. The 7 topologies of footbridges considered in this study. Simplex S1 and S2 (S2 is a similar to S1, but with a sinusoidal deck), quadruplex Q1, quadruplex Q2, pentaplex P1, pentaplex P2, hexaplex H1, hexaplex H2.

3. Design methodology using morphological indicators

It has been proven (Latteur et al, 2017) that, for a given structure composed of S elementary tensegrity modules of span L, height H, width D, composed of materials of mechanical characteristics ($E_c, \sigma_c, E_s, \sigma_s$), subjected to an external load $\tilde{\mathbf{F}} = F\tilde{\mathbf{f}}$ and a pre-stress scenario $\tilde{\mathbf{P}} = \beta F\tilde{\mathbf{p}}$, and with struts and cables designed according to (1a, 1b):

- The deflection at mid span (or anywhere else) δ/L only depends on 7 dimensionless numbers, according to:

$$\frac{\delta}{L} = f\left(\frac{L}{H}, \frac{L}{D}, \Psi, \frac{E_c}{\sigma_c}, \frac{E_s}{\sigma_s}, S, \beta\tilde{\mathbf{p}}\right) \tag{2a}$$

- The volume V of materials, defined by its *indicator of volume* W, only depends on the same 7 dimensionless numbers and on $u = \sigma_c/\sigma_s$, according to:

$$W = \frac{\sigma_s V}{FL} = f\left(\frac{L}{H}, \frac{L}{D}, \Psi, \frac{E_c}{\sigma_c}, \frac{E_s}{\sigma_s}, S, \beta\tilde{\mathbf{p}}, u\right) \tag{2b}$$

Where Ψ is the *indicator of buckling* (Latteur et al, 2000, 2001) such that $\Psi = \sigma_s L \big/ \sqrt{qE_s F}$.

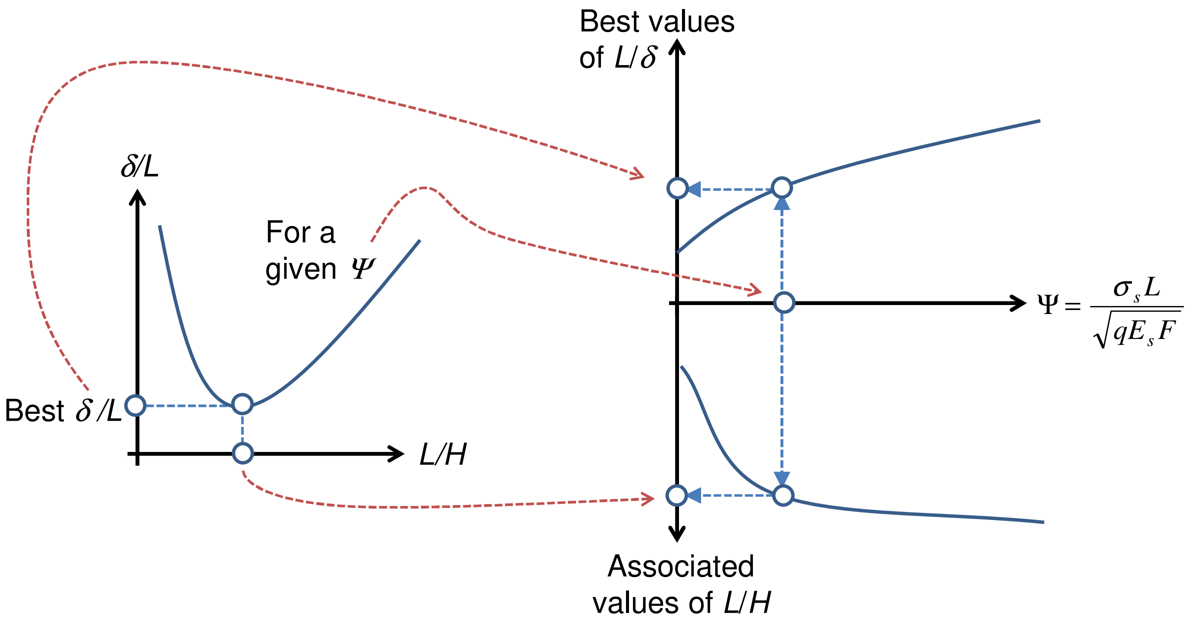

Fig. 11. For a given practical case related to a given value of ψ, the *efficiency curve* (right graph) gives the best value L/H, and the associated (best) value δ/L (or L/δ).

This methodology allows to easily finding the stiffest or the lightest structure thanks to the *efficiency curves* shown in figure 11. Indeed, assuming that:

- The span L and the load case $\tilde{\mathbf{F}}$ of a given project are known;
- The materials are chosen ($E_c/\sigma_c, E_s/\sigma_s, u$);
- The pre-stress level and state, respectively, β and $\tilde{\mathbf{p}}$ are arbitrarily fixed as explained in the assumptions;
- D is proportional to H for a given topology of structures,

Relations (2a) and (2b) become, for a given number S of elementary modules:

$$\frac{\delta}{L} = f\left(\frac{L}{H}, \Psi\right) \quad \text{and} \quad W = \frac{\sigma_s V}{FL} = f\left(\frac{L}{H}, \Psi\right) \tag{3a, 3b}$$

Using relations (3a,3b), the optimization and the design process are thus greatly simplified, since the deflection δ/L and the *indicator of volume* W only depend on the 2 parameters L/H and Ψ. This is illustrated in figure 11 for the deflection δ/L.

The goal of this article is to compare the structural performances (stiffness and volume) of the 7 topologies of structures shown in figure 10 thanks to the *efficiency curves,* and to discuss the relevance of such structures for footbridges applications.

The developments of (Latteur et al, 2017) only consider the external load case $\tilde{\mathbf{F}}$ for the optimization process. This means that a structure which is optimized only for the external load case $\tilde{\mathbf{F}}$ might not be optimum anymore when the self-weight $\tilde{\mathbf{G}}$ is combined to $\tilde{\mathbf{F}}$, since self-weight can reach a non-negligible percentage of $\tilde{\mathbf{F}}$ for large spans. However, a solution can be found as explained below.

It is assumed that gravity is acting in the Z direction and that the bending of the elements due to their self-weight can be neglected. For any structure, self-weight can thus be taken into account by assuming that each strut or cable connected to a node adds to this node a vertical load equal to the half of its own self-weight. The process is of course iterative : given an external load $\tilde{\mathbf{F}}$, one can calculate the self-weight and its associated self-weight equivalent load case $\tilde{\mathbf{G}}$, which leads to a new calculation of the structure subjected to ($\tilde{\mathbf{F}} + \tilde{\mathbf{G}}$), and so on until de results converge towards a final value of $\tilde{\mathbf{G}}$.

Taking self-weight into account keeps the design methodology described in (Latteur et al, 2017) valid. Indeed:

Half of the self-weight of a strut or cable of index *i* of volume V_i is equal to: $\rho V_i/2$.

Given the fact that the part W_i of the indicator of volume related to an element *i* of a structure subjected to $\tilde{\mathbf{F}}$ is equal to:

$$W_i = \frac{\sigma_s V_i}{FL} = f\left(\frac{L}{H}, \frac{L}{D}, \Psi, \frac{E_c}{\sigma_c}, \frac{E_s}{\sigma_s}, S, \beta\tilde{\mathbf{p}}, u\right)$$, one gets:

$$\frac{\rho V_i}{2} = \frac{\rho L}{\sigma} * \frac{F}{2} * f\left(\frac{L}{H}, \frac{L}{D}, \Psi, \frac{E_c}{\sigma_c}, \frac{E_s}{\sigma_s}, S, \beta\tilde{\mathbf{p}}, u\right)$$

If $\Phi_c=\rho_c L/\sigma_c$ *and* $\Phi_s=\rho_s L/\sigma_s$ are defined, respectively, as the *indicators of self-weight* (Latteur, 2000) of the cables and the struts, upper relations show that self-weight $\tilde{\mathbf{G}}$ coming from an external load $\tilde{\mathbf{F}}$ is acting as a new load case proportional to F and which only depends on parameters L/H, L/D, Ψ, E_c/σ_c, E_s/σ_s, S, $\beta\tilde{\mathbf{p}}$, u, Φ_c, Φ_s . This allows to extend relations (2a) and (2b) as follows:

$$\frac{\delta}{L} = f\left(\frac{L}{H}, \frac{L}{D}, \Psi, \frac{E_c}{\sigma_c}, \frac{E_s}{\sigma_s}, S, \beta\tilde{\mathbf{p}}, u, \Phi_c, \Phi_s\right) \quad (4a)$$

$$W = \frac{\sigma_s V}{FL} = f\left(\frac{L}{H}, \frac{L}{D}, \Psi, \frac{E_c}{\sigma_c}, \frac{E_s}{\sigma_s}, S, \beta\tilde{\mathbf{p}}, u, \Phi_c, \Phi_s\right) \quad (4b)$$

It is interesting to note that taking $\tilde{\mathbf{G}}$ into account makes this time δ/L dependent on factor u .

Note that for steel with E=210 GPa, σ=237 MPa, ρ=77kN/m^3 , the indicator of self-weight is the same for cables and struts and is equal to Φ=0,325.10^{-6}L (L in [mm]). For spans limited to 100 m, the indicator of self-weight is thus limited to 325.10^{-4}. Furthermore, previous study (Latteur et. al, 2000) has shown that values of Ψ higher than 100 are related to very heavy and low efficient structures.

A very interesting consequence of the existence of the indicator of self-weight Φ is that it can be used to quantify the ratio between the total self-weight ρV of the structure and the total external load F:

$$\frac{\rho V}{F}=\rho\frac{V}{F}=\rho\frac{WL}{\sigma_s}=\Phi_s W=f\left(\frac{L}{H},\frac{L}{D},\Psi,\frac{E_c}{\sigma_c},\frac{E_s}{\sigma_s},S,\beta\tilde{\mathbf{p}},u,\Phi_c,\Phi_s\right)$$

4. Numerical algorithm

Figure 12 summarizes the algorithm used by the software that authors developed, already partly presented in (Latteur et al, 2017) but here modified to take into account self-weight as a load case added to the external load case. The code has been developed in Python and figure 12 shows the numerical optimization process that leads to the results presented further.

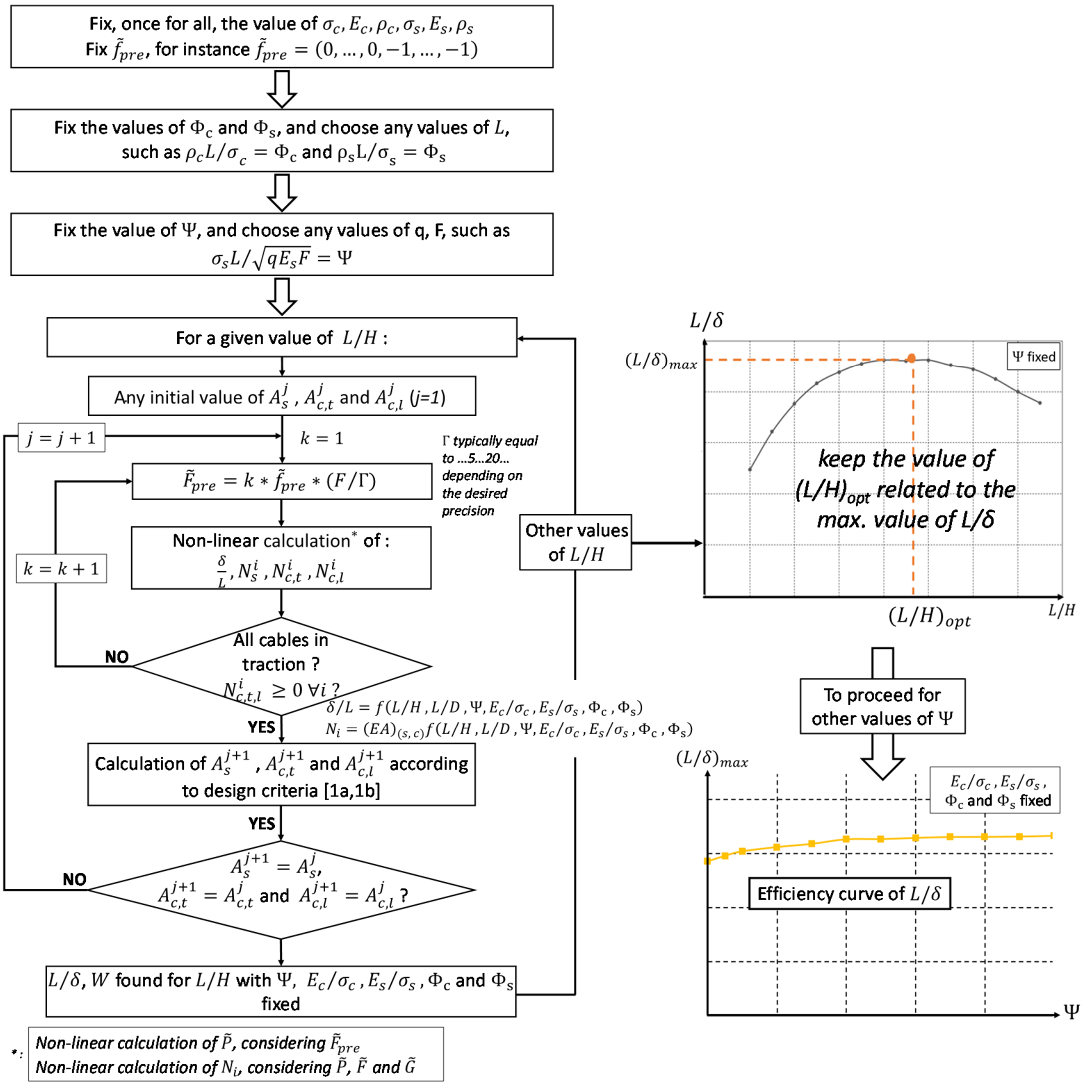

Fig. 12. Numerical algorithm used to find the value of (L/H, $(L/\delta)_{max}$) related to given values of Ψ and of Φ.

Algorithm of figure 12 can be summarized as followed (for a given number S of elementary tensegrity modules):

- Materials are chosen, in this article, steel ($E/\sigma= E_c/\sigma_c$=886 and u=1) is considered;
- The values of Ψ, Φ and L/H are first chosen within the following ranges : $0\leq\psi\leq100$, $0\leq\Phi\leq325.10^{-4}$, $0<L/H\leq15$;
- The value of Φ gives automatically the value of L (Φ=0,325.10^{-6}*L);
- Factors q and F are arbitrarily chosen in order to respect the value of Ψ:

$$\Psi=\sigma L/\sqrt{qEF}\rightarrow qF=(\sigma L/\Psi)^2/E\ ;$$

- The value of L/H gives the value of H ;
- Calculation of δ/L at mid span (or W) for those precise values of Ψ, Φ and L/H;
- If the process is repeated for each value of L/H, the couple (best L/H, best δ/L) or (best L/H, best W) can be found for each value of Ψ, and reported on an efficiency curve. One efficiency curve is related to a single value of Φ (or the span L) and a single value of E/σ;
- The same algorithm can be used for several values of S, for instance 2, 3, 4, 5, 6, etc.

5. Results for family S1-S2 (simplex)

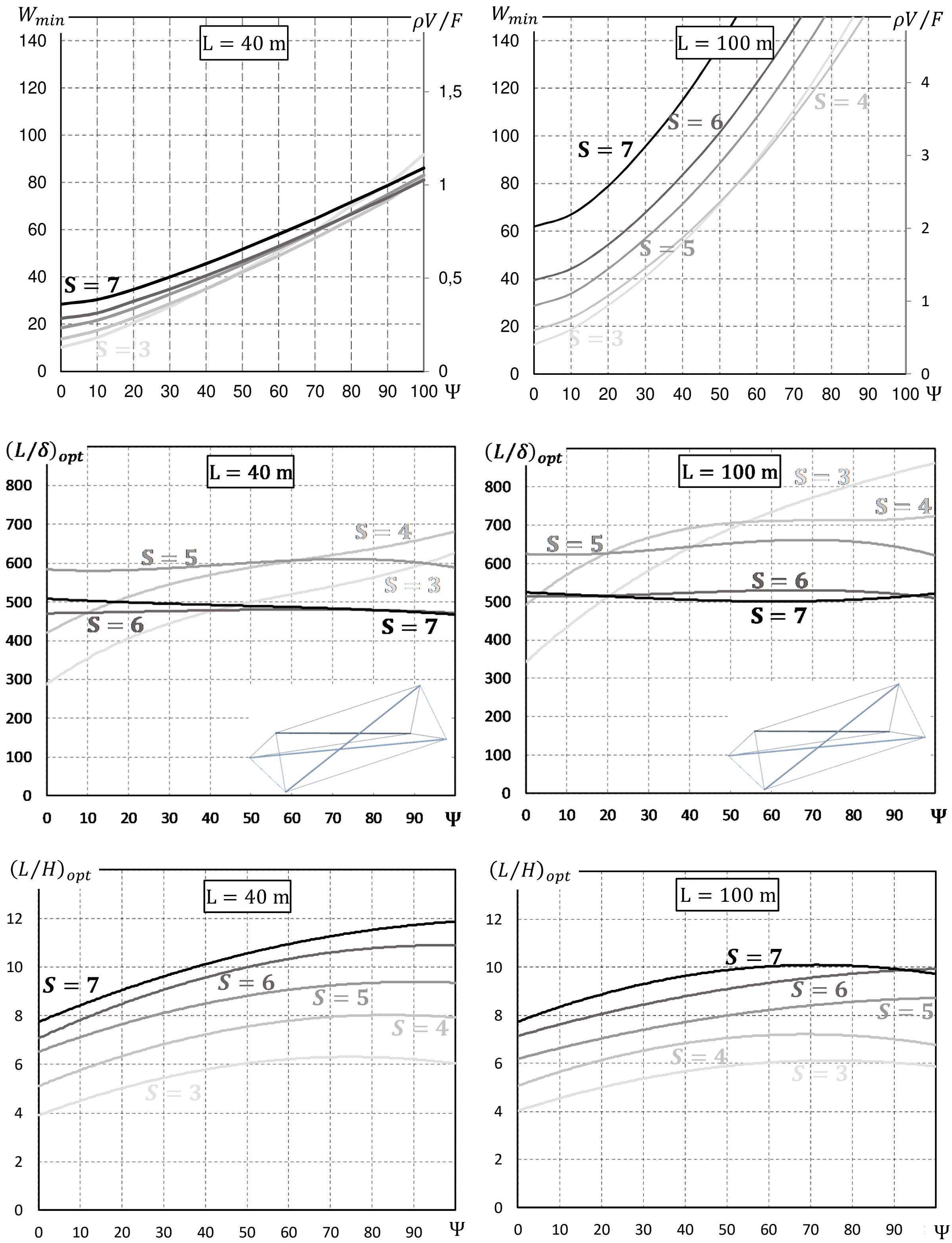

Fig. 13. Efficiency curves of W for L=40m (Φ=130.10^{-4}) and for L=100m (Φ=325.10^{-4}). Above: efficiency curves of W and $\rho V/F$. Middle: associated values of L/δ. Below: associated values of L/H.

The possible information resulting from the analysis of the computations done for each of the 7 topologies (figure 10) is very dense: the variations of δ/L and W in function of L/H for a fixed Ψ, the efficiency curves of δ/L associated with the corresponding (and not necessarily optimum) values of W, or the reverse situation where the efficiency curves of W are drawn, in association with the corresponding (and not necessarily optimum) values of δ/L, etc. This can be done independently for each topology, or as a comparison between all of them.

The criterion related to volume, linked to self-weight and thus to the cost of the structure, is very relevant. Indeed, this research tends to show that these structures are very stiff, but are heavier than more classical structures as trusses for instance. For a practical project, the criterion linked to the volume (or self-weight or quantity of materials) is thus very relevant. Moreover, our studies showed that the optimum structures in terms of volume are not very far from the optimum structures in terms of deflection.

Hence, the aim of this article is to prove the feasibility of such footbridges. Therefore, it seems relevant and sufficient to consider the lightest structures (efficiency curves related to W) and to show that the associated values of δ/L remain acceptable. This is the reason why the results shown in this article will mainly focus on the efficiency curves of W and not of δ/L.

Figure 13 leads to the following comments (curves S=2 show a bad efficiency in terms of volume and deflection and were not drawn):

- The minimum volume of materials V_{min} (or W_{min}) increases with the growing values of the indicator of buckling Ψ and of the indicator of self-weight Φ (or the span L);
- At the contrary, the associated deflection δ/L shows small variations with Ψ and Φ (in particular for S>4);
- Globally, whatever the value of Ψ, the minimum volume of materials V_{min} (or W_{min}) increases with the number of elementary tensegrity modules S;
- S=5 always shows a very good stiffness L/δ above 550. Moreover, since the deflection δ is also due to self-weight, the deflection under live loads only is much better than L/550. The corresponding values of L/H are always between 6 and 10;
- S=3 and S=4 have a better stiffness L/δ than S=5 when Φ (or the span L) and Ψ increase;
- The choice $3 \leq S \leq 5$ is always the best whatever the values of Ψ and Φ.

However, figure 13 does not exclude solutions with an insufficient stiffness ($\delta = L/500$ is considered as a maximum in this article, as discussed in section "Allowable deflections"), an insufficient headroom h_r for pedestrians or an insufficient deck width b (2m for both seems to be a minimum). Imposing a minimum value for h_r and b is equivalent to impose a maximum value of ratio L/H, noted $(L/H)_{limit}$. Figure 13 should thus be corrected according to the methodology described in figure 14:

- Case 1 : the solution with minimum volume corresponds to $L/\delta \geq 500$: ok;
- Cases 2 and 3 : the solution with the minimum volume is out of the range of sufficient stiffness. However, a solution exists with $L/\delta = 500$ but need higher volume of material W_{min};
- Case 4 : no solution with $L/\delta \geq 500$ exist;
- Case 5 : is similar to case 1 but in this case a non-optimum solution has to be considered to ensure sufficient headroom and deck width combined with $L/\delta \geq 500$;
- Case 6 : is similar to case 1 but in this case no solution can be found with the 3 criteria respected.

Figure 15 is a correction of figure 13 according to figure 14 in the way that it shows, for spans respectively equal to 40m and 100m, the "optimum" structures of topology S2 combining $\delta \leq 500$, $h_r \geq 2m$ and $b \geq 2m$. All the other situations have been rejected. On figure 15 are pointed out two S2 structures related to Ψ=48 and, respectively, S=4 and S=5 . The schemas of these structures are shown in figure 25.

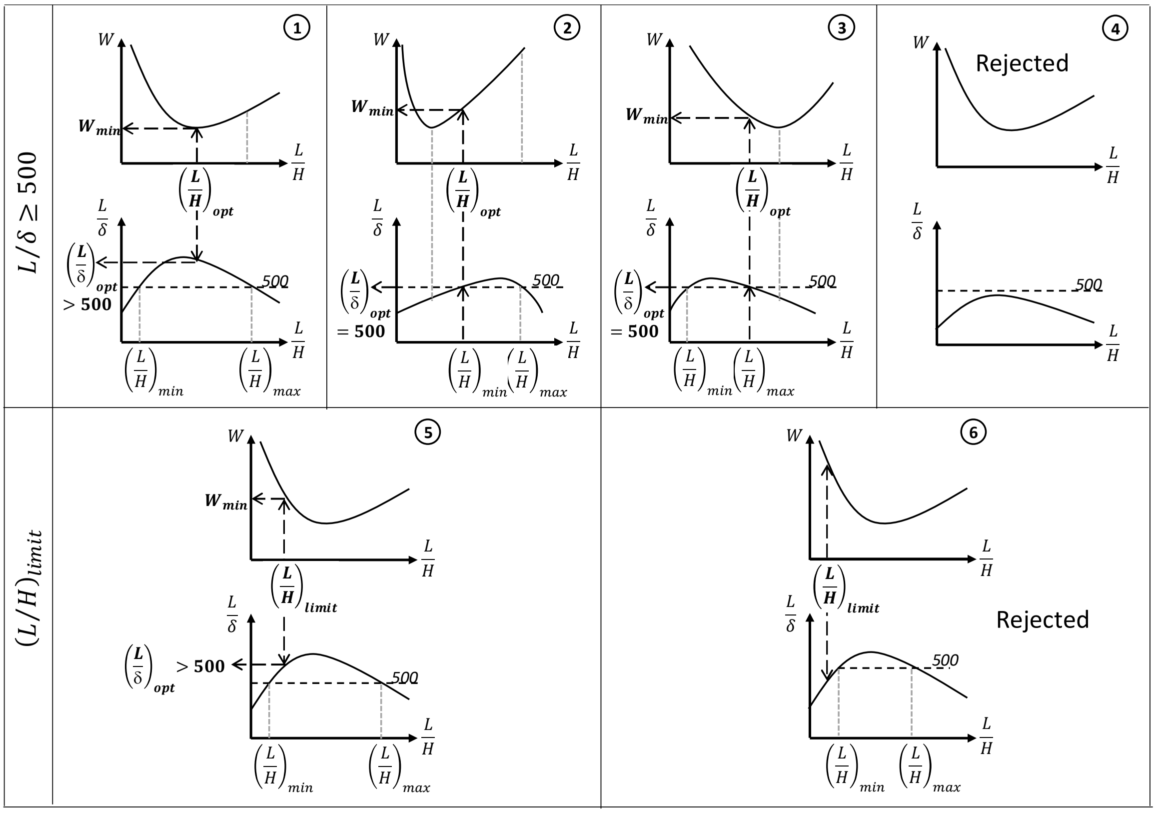

Fig. 14. Construction of efficiency curve of W by selecting, for a fixed Ψ, the best L/H with the constraints $\delta \leq L/500$, $h_r \geq 2$ m and $b \geq 2$ m.

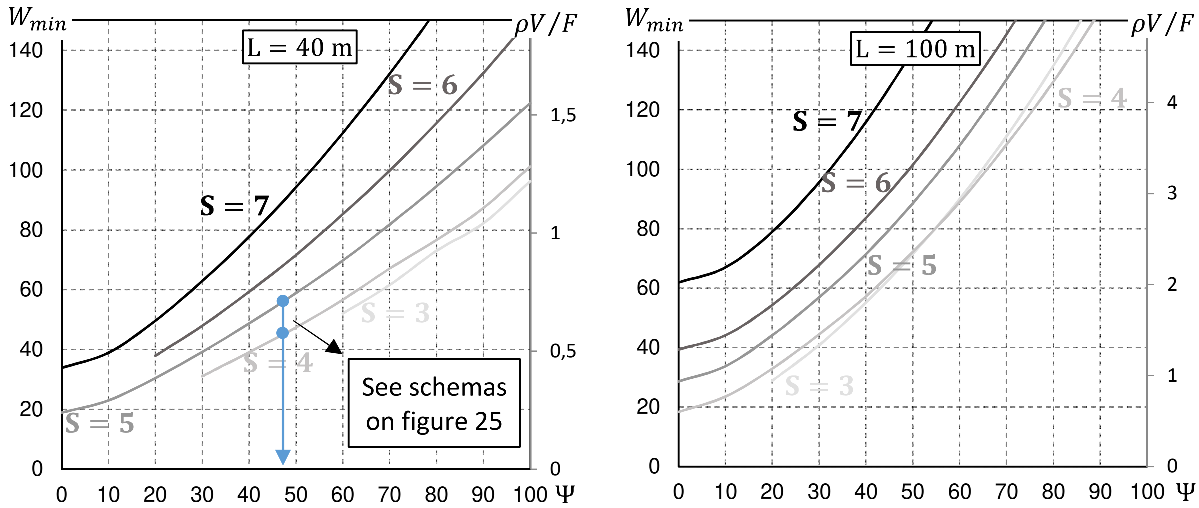

Fig. 15. Correction of figure 13 with the constraints $\delta \leq L/500$, $h_r \geq 2$m and $b \geq 2$m (topology S2). All the other cases have been rejected. Left figure: L=40m, right figure: L=100m.

6. Study of the other topologies Q1, Q2, P1, P2, H1 and H2

After previous section detailing the family S1/S2 composed of simplex modules, this section summarizes the results for the other topologies. To make the comparison easier, the curve related to topology S1/S2-*S*=5 has been systematically added to the figures below, in dashed lines. In this section, the optimum values are given with no constraint on h_r and b, at the contrary of section "General comparison of the 7 topologies".

6.1. Family Q1

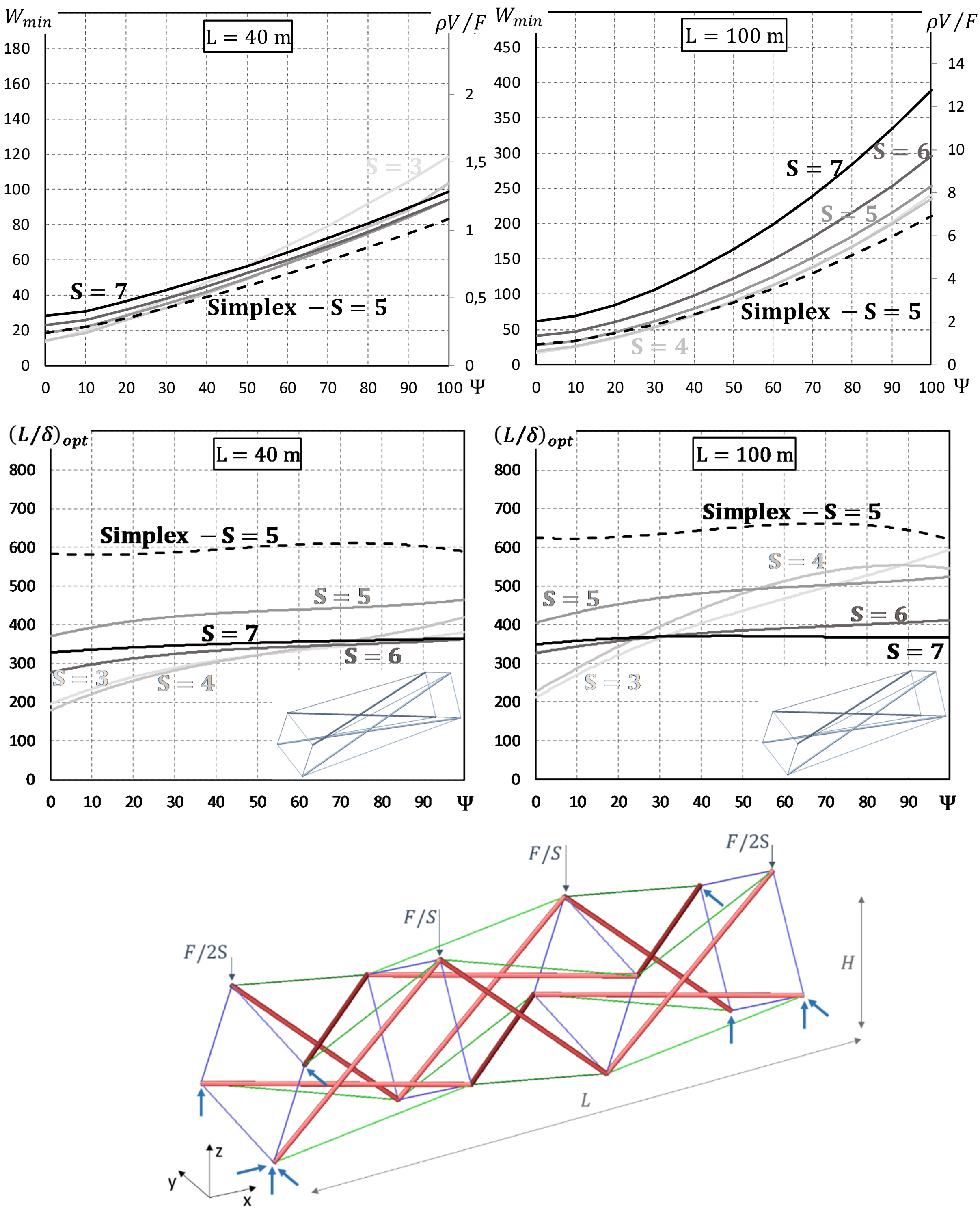

Fig. 16. Family Q1: composed of quadruplex of type 1.

This family has a stiffness that seldom reaches L/δ=500, while the simplex family shows a better stiffness around L/δ=600 whatever the span or the value of Ψ. For *S*=6 and *S*=7, the stiffness is never better than L/δ=400, whatever the span and the values of Ψ. In terms of stiffness, *S*=5 is always better than all the others, except for large spans and large values of Ψ, where *S*=3 and *S*=4 can slightly overtake L/δ=500.

The volume is always higher than for the simplex family, except for low values of Ψ, whatever the span, but only for *S*=3 and *S*=4. However, the gain in volume with respect to the simplex family is insignificant and, furthermore, small values of Ψ for *S*=3 and *S*=4 correspond to a very bad stiffness.

As a conclusion, excluding considerations linked to the headroom, this family of structures is never more advantageous than the simplex family, even if choices like *S*=3 and *S*=4 for large spans and high values of Ψ, or *S*=5 can lead to acceptable solutions.

6.2. Family Q2

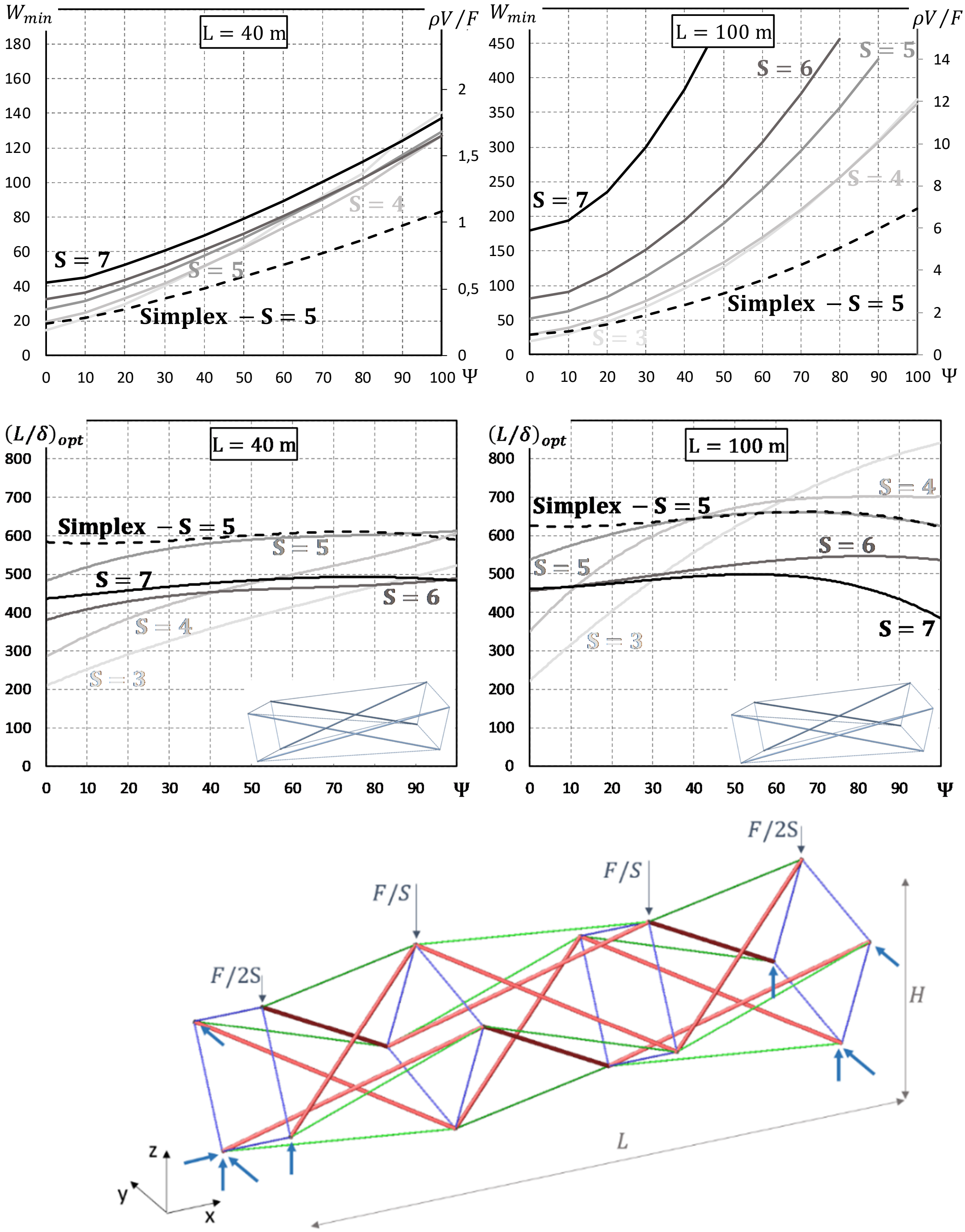

Fig. 17. Family Q2: composed of quadruplex of type 2.

This family shows a better behavior than the preceding one regarding the stiffness and many solutions with deflections better than $L/500$ can be found. In particular, the solution *S*=5 is almost always the best regarding the stiffness, and equivalent to the simplex family. However, for similar performances regarding the deflection, the volume of materials is much higher than for the simplex family and the volume increases very quickly up to irrelevant values. There is an exception for *S*=3 and *S*=4 and for very small values of Ψ, but their lack of stiffness disqualifies them. As a conclusion, this family of structures is only interesting with S=5 and for small values of Ψ, or for reasons linked to the headroom.

6.3. Family P1

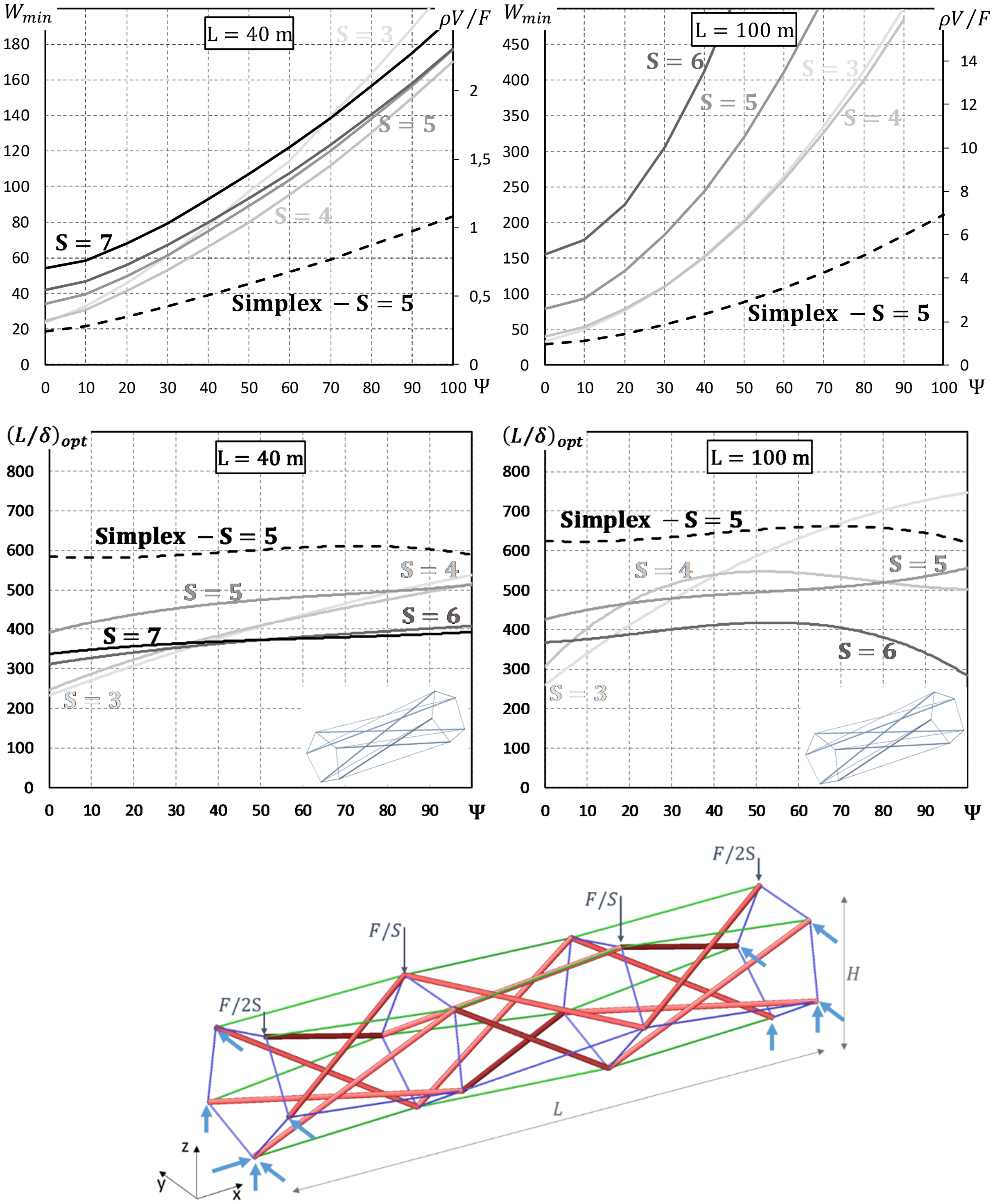

Fig. 18. Family P1: composed of pentaplex of type 1.

These structures are always heavier than the ones of the simplex family, whatever the span and the value of Ψ. For values of Ψ above 50, the volume is at least doubled, in comparison with the simplex family. In terms of volume, the only acceptable solution could be related to S=4 (and even *S*=3) only for values of Ψ lower than 20, but these situations correspond to a small stiffness.

The conclusion is that this family should probably be rejected for most cases.

6.4. Family P2

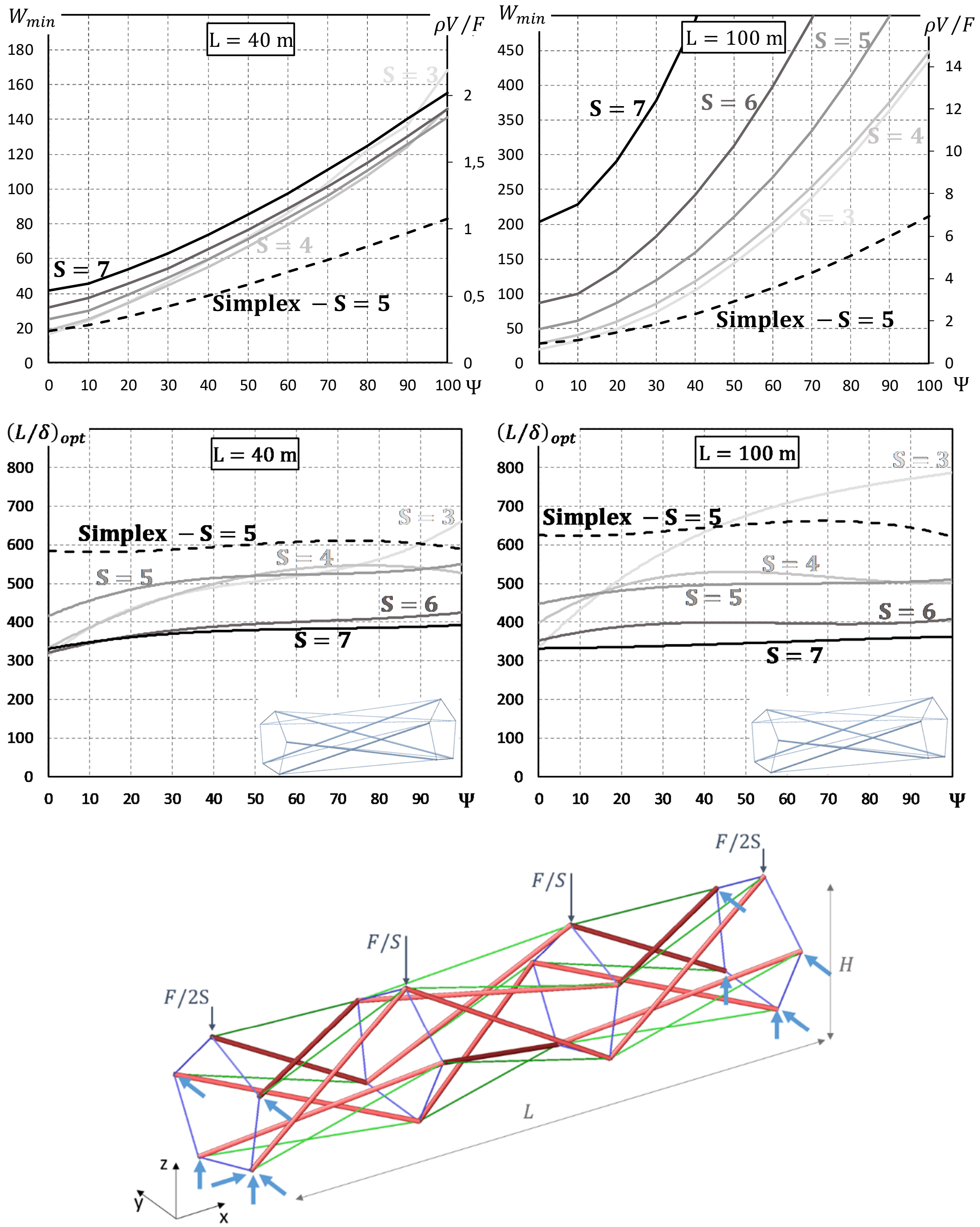

Fig. 19. Family P2: composed of pentaplex of type 2.

The results for this family are very similar to the previous one P1. In terms of stiffness, *S*=3, *S*=4 and *S*=5 are acceptable and slightly better than for family P1. However, the volume grows quickly after *Ψ*=40, with unreasonable solutions, in particular for large spans.

As a conclusion, excluding considerations linked to the headroom, this family of structures is never more advantageous than the simplex family, even if choices like *S*=3, *S*=4 and *S*=5 for small values of *Ψ* can lead to acceptable solutions.

6.5. Family H1

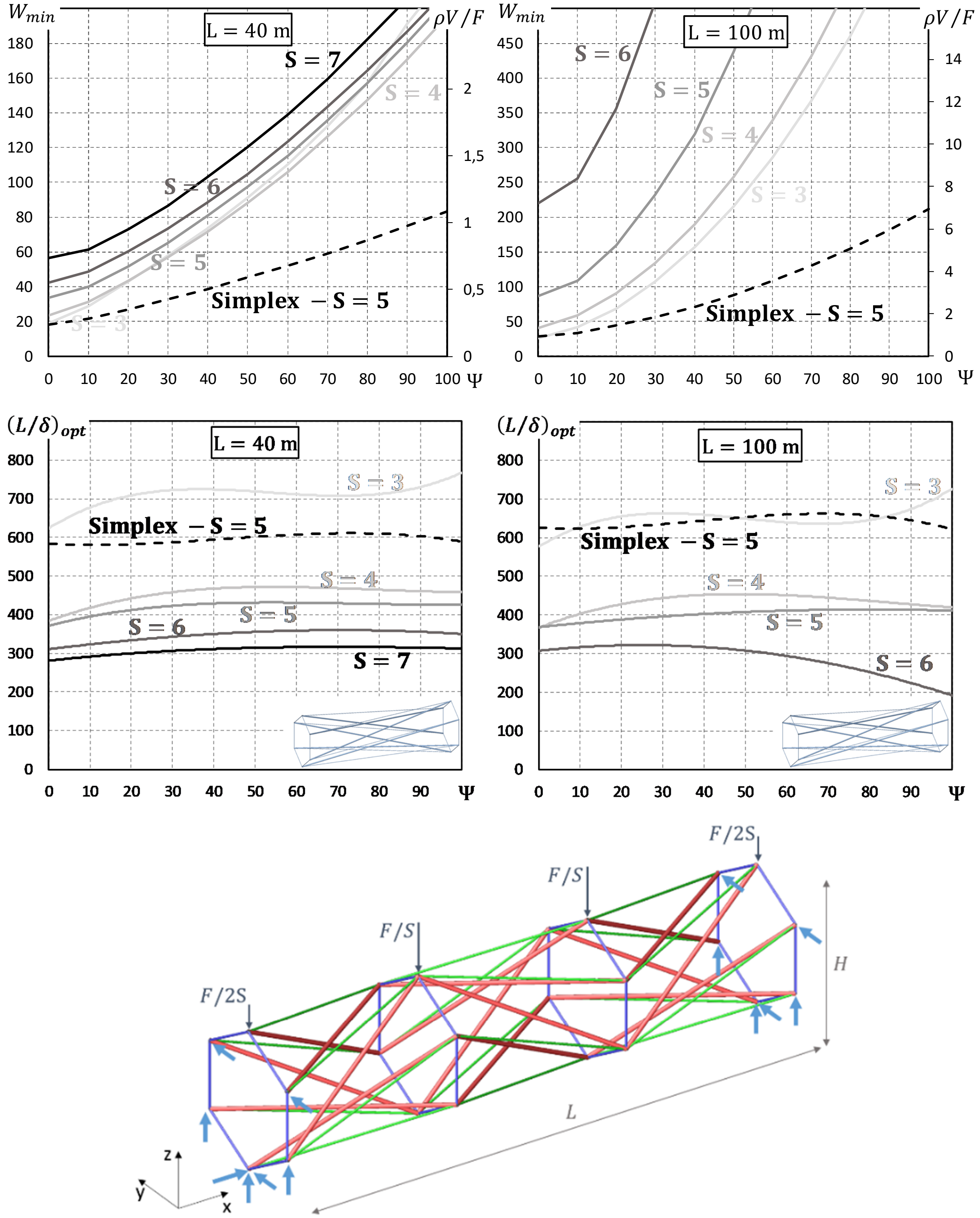

Fig. 20. Family H1: composed of hexaplex of type 1.

This family is interesting for *S*=3, with good deflection performances, even sometimes better than the S1/S2 family. However, the volume remains much higher, in particular for values of Ψ>30. Its interest is thus limited to structures with short or middle spans associated to a low value of Ψ, otherwise the volume, and thus the cost, becomes unreasonable. Solutions also exist with *S*=4 or *S*=5, but with a higher volume than *S*=3.

6.6. Family H2

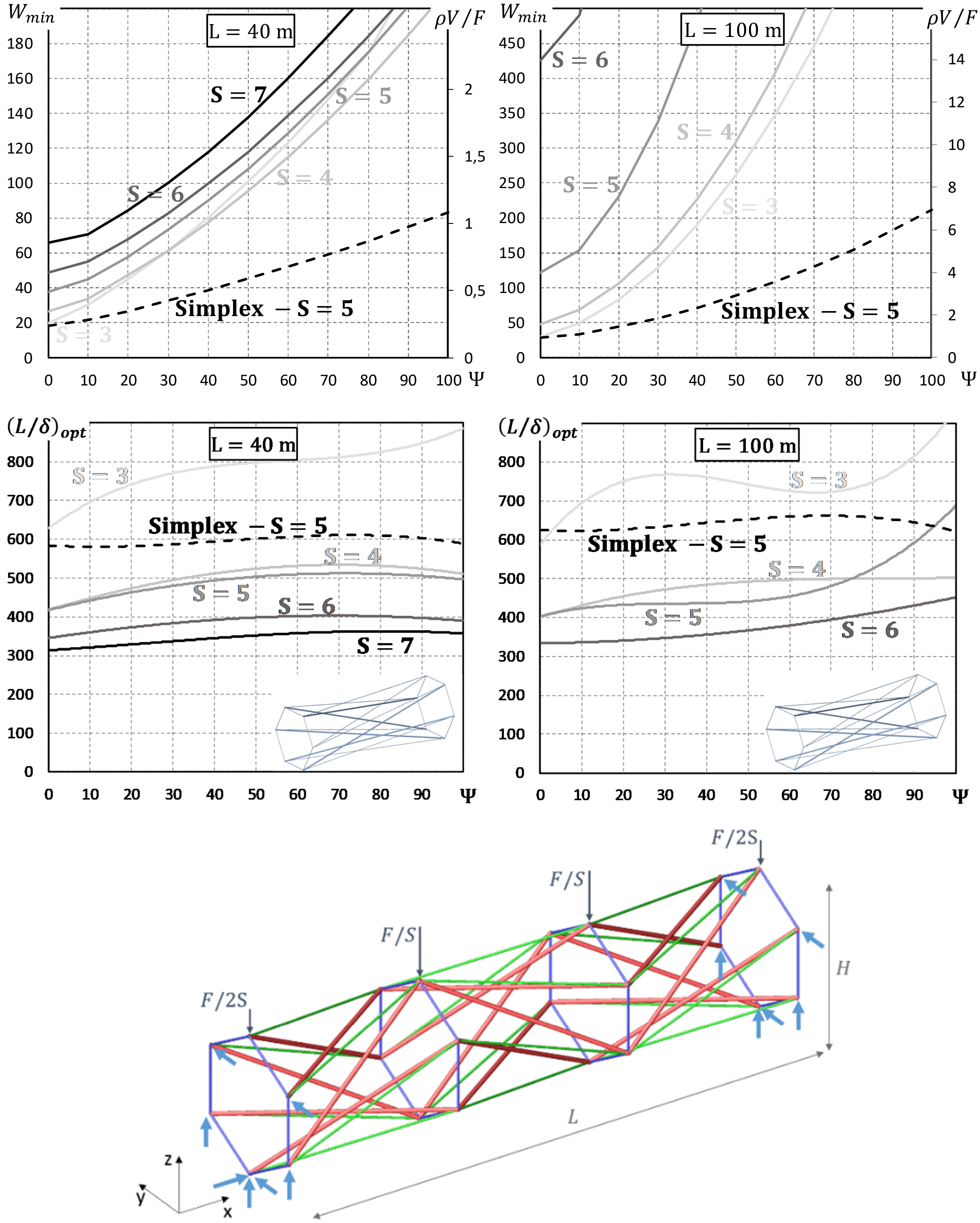

Fig. 21. Family H2: composed of hexaplex of type 2.

This family shows very similar characteristics than family H1 and similar conclusions can be drawn. *S*=3 shows an excellent stiffness, always better than the simplex family. However, for values of Ψ greater than 20, the volume grows unreasonably. As a conclusion, solutions exist with *S*=3, *S*=4 and *S*=5, but only when Ψ is small.

7. General comparison of the 7 topologies

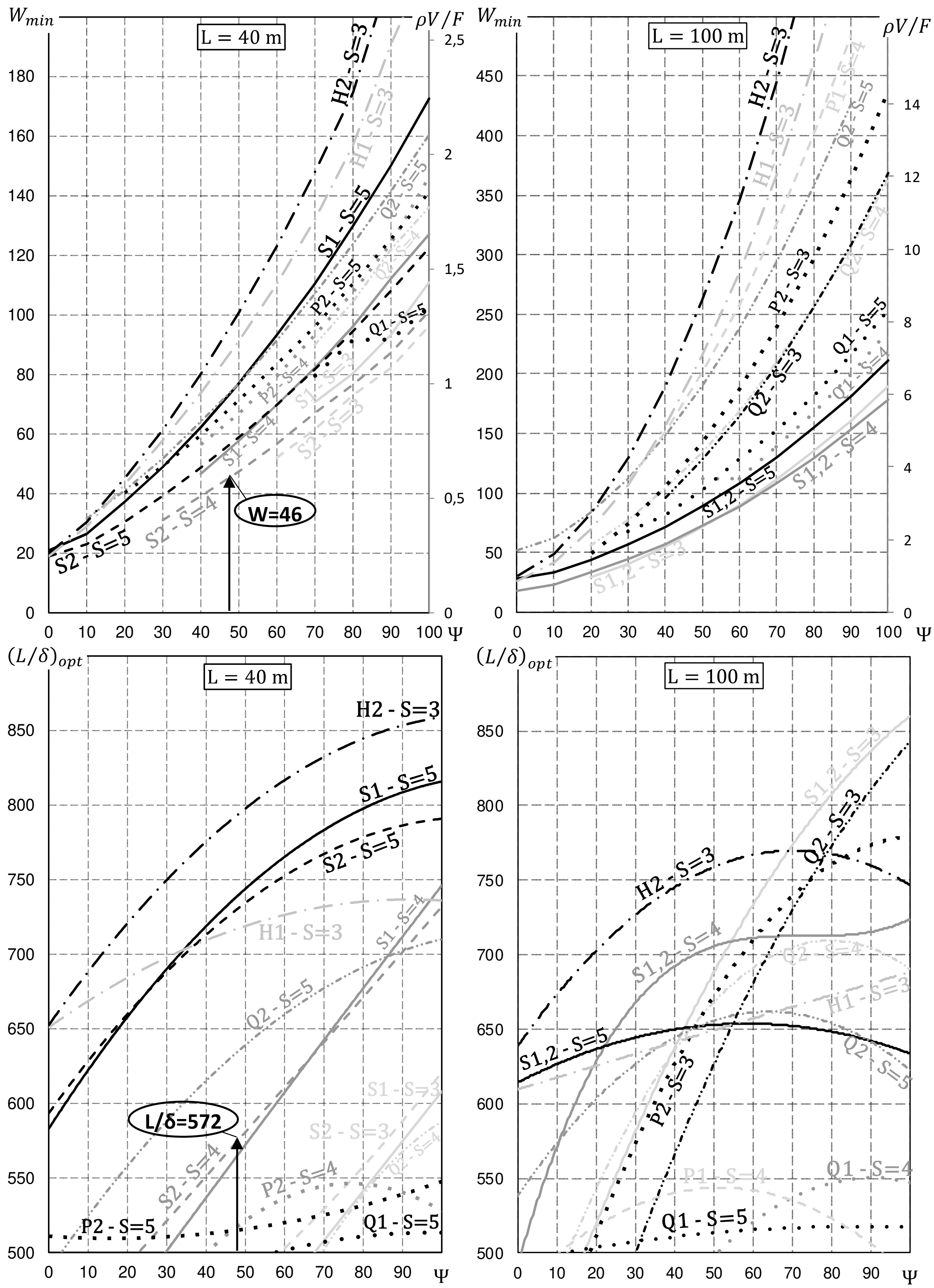

Fig. 22. Comparison of the different families for *L*=40m (left) and *L*=100m (right). Only the structures with $\delta \leq L/500$ (deck's width) and $h_r \geq 2$m (headroom for pedestrians) have been kept.

This section brings together the results presented in sections "Results for family S1-S2 (simplex)" and "Study of the other topologies Q1, Q2, P1, P2, H1 and H2" in order to make a general comparison. Only the following structures with $\delta \leq L/500$, $h_r \geq 2$m (headroom for pedestrians) and $b \geq 2$m (deck's width) have been kept:

- Families S1 and S2 (simplex) with S=3, S=4 and S=5;
- Family Q1 (quadruplex of type 1) with S=4 and S=5;
- Family Q2 (quadruplex of type 2) with S=3, S=4 and S=5;
- Family P1 (pentaplex of type 1) with S=4;
- Family P2 (pentaplex of type 2) with S=3, S=4 and S=5;
- Family H1 (hexaplex of type 1) with S=3;
- Family H2 (hexaplex of type 2) with S=3;

Ψ	1		2		3		4		5	
	Wmin	(L/δ)opt	Wmin	(L/δ)opt	Wmin	(L/δ)opt	Wmin	(L/δ)opt	Wmin	(L/δ)opt
0	18,9	592	19	595	20	621				
	S2 - S=5, L/H=5, ρV/F=25%		H1 - S=3, L/H=3, ρV/F=25%		H2 - S=3, L/H=3, ρV/F=26%					
10	23	627	29	682	30,4	715				
	S2 - S=5, L/H=5, ρV/F=30%		H1 - S=3, L/H=4, ρV/F=38%		H2 - S=3, L/H=4, ρV/F=40%					
20	30,5	666	37,3	670	43	754	45,2	785		
	S2 - S=5, L/H=5, ρV/F=40%		S1 - S=5, L/H=4, ρV/F=49%		H1 - S=3, L/H=4, ρV/F=56%		H2 - S=3, L/H=4, ρV/F=59%			
30	31,1	519	39,2	696	49	696	57,8	698	61,4	742
	S2 - S=4, L/H=5, ρV/F=41%		S2 - S=5, L/H=5, ρV/F=51%		S1 - S=5, L/H=4, ρV/F=64%		H1 - S=3, L/H=5, ρV/F=76%		H2 - S=3, L/H=5, ρV/F=80%	
40	39,1	554	48,7	717	62,3	720	80,3	774		
	S2 - S=4, L/H=5, ρV/F=51%		S2 - S=5, L/H=5, ρV/F=64%		S1 - S=5, L/H=4, ρV/F=82%		H2 - S=3, L/H=5, ρV/F=105%			
50	47,4	579	58,9	733	77	742	100,8	793		
	S2 - S=4, L/H=5, ρV/F=62%		S2 - S=5, L/H=5, ρV/F=77%		S1 - S=5, L/H=4, ρV/F=101%		H2 - S=3, L/H=5, ρV/F=132%			
60	52,1	502	56,7	612	69,9	747	93,3	763	123,1	805
	S2 - S=3, L/H=5, ρV/F=68%		S2 - S=4, L/H=5, ρV/F=74%		S2 - S=5, L/H=5, ρV/F=92%		S1 - S=5, L/H=4, ρV/F=122%		H2 - S=3, L/H=5, ρV/F=161%	
70	61,6	528	67	649	81,8	763	110,5	778	147,9	816
	S2 - S=3, L/H=5, ρV/F=81%		S2 - S=4, L/H=5, ρV/F=88%		S2 - S=5, L/H=5, ρV/F=107%		S1 - S=5, L/H=4, ρV/F=145%		H2 - S=3, L/H=5, ρV/F=194%	
80	73	569	76,7	667	94,6	775	129,8	794	174,5	823
	S2 - S=3, L/H=5, ρV/F=96%		S2 - S=4, L/H=5, ρV/F=101%		S2 - S=5, L/H=5, ρV/F=124%		S1 - S=5, L/H=4, ρV/F=170%		H2 - S=3, L/H=5, ρV/F=229%	
90	82,2	575	87,3	690	108,2	787	150,2	802	215,6	867
	S2 - S=3, L/H=5, ρV/F=108%		S2 - S=4, L/H=5, ρV/F=114%		S2 - S=5, L/H=5, ρV/F=142%		S1 - S=5, L/H=4, ρV/F=197%		H2 - S=3, L/H=5, ρV/F=283%	
100	96,3	626	101,2	740	122,4	796	172,6	822	249,7	873
	S2 - S=3, L/H=5, ρV/F=126%		S2 - S=4, L/H=5, ρV/F=133%		S2 - S=5, L/H=5, ρV/F=160%		S1 - S=5, L/H=4, ρV/F=226%		H2 - S=3, L/H=5, ρV/F=327%	

Table 1. Comparison of the different families for *L*=40m.

Ψ	1		2		3		4	
	Wmin	(L/δ)opt	Wmin	(L/δ)opt	Wmin	(L/δ)opt	Wmin	(L/δ)opt
0	18,4	502	26,1	576	30	616		
	S1,2 - S=4, L/H=5, ρV/F=60%		H1 - S=3, L/H=3, ρV/F=86%		H2 - S=3, L/H=3, ρV/F=98%			
10	23,5	564	41,5	615	48,9	675		
	S1,2 - S=4, L/H=6, ρV/F=77%		H1 - S=3, L/H=4, ρV/F=136%		H2 - S=3, L/H=3, ρV/F=160%			
20	28,9	519	32,9	631	69	661	82,7	742
	S1,2 - S=3, L/H=5, ρV/F=95%		S1,2 - S=4, L/H=6, ρV/F=108%		H1 - S=3, L/H=4, ρV/F=226%		H2 - S=3, L/H=4, ρV/F=271%	
30	40,8	579	44,5	680	108	689	129,5	778
	S1,2 - S=3, L/H=5, ρV/F=134%		S1,2 - S=4, L/H=7, ρV/F=146%		H1 - S=3, L/H=4, ρV/F=354%		H2 - S=3, L/H=4, ρV/F=424%	
40	55,2	641	57,3	691	189,4	799		
	S1,2 - S=3, L/H=5, ρV/F=181%		S1,2 - S=4, L/H=7, ρV/F=188%		H2 - S=3, L/H=4, ρV/F=621%			
50	71,5	690	72,2	701	261,9	718		
	S1,2 - S=3, L/H=6, ρV/F=234%		S1,2 - S=4, L/H=7, ρV/F=237%		H2 - S=3, L/H=4, ρV/F=858%			
60	89	706	90	733				
	S1,2 - S=4, L/H=7, ρV/F=292%		S1,2 - S=3, L/H=6, ρV/F=295%					
70	108,3	712	111,1	772				
	S1,2 - S=4, L/H=7, ρV/F=355%		S1,2 - S=3, L/H=6, ρV/F=364%					
80	129,5	715	134,8	807				
	S1,2 - S=4, L/H=7, ρV/F=424%		S1,2 - S=3, L/H=6, ρV/F=442%					
90	153,3	719	161,3	837				
	S1,2 - S=4, L/H=7, ρV/F=502%		S1,2 - S=3, L/H=6, ρV/F=529%					
100	178,8	721	189,8	861				
	S1,2 - S=4, L/H=7, ρV/F=586%		S1,2 - S=3, L/H=6, ρV/F=622%					

Table 2. Comparison of the different families for *L*=100m.

Tables 1 and 2 summarize the best structures of figure 22 in terms of volume, with the associated stiffness L/δ and relative self-weight $\rho V/F$. Structures are sorted from left to right according to their indicators of volume W in ascending order, keeping only those that show a better stiffness L/δ than the previous lighter structures.

Concerning the volume, Figure 22 and tables 1 and 2 suggest that:

- The H2/S=3 family is always heavier than all the others;
- The simplex family with S=3, S=4 or S=5 always offers the lightest solutions, whatever the span or the value of Ψ;
- For small and middle spans, the simplex S2 solution is always better, and, for growing values of Ψ, the number of tensegrity modules has to decrease progressively from S=5 to S=3;
- For large spans, the simplex S1 (or S2) with 3 or 4 modules is always the lightest solution;
- Family Q1 also offers competitive solutions, whatever the span, for S=4 and S=5;
- All other families show unreasonable volumes, growing fast when the span or the value of Ψ grow;
- For the lightest structures (family S1,S2), the ratio self-weight over total live load $\rho V/F$ is between 25% and 125% for L=40m, and between 75% and 600% for L=100m, depending on the values of Ψ.

Concerning the stiffness, Figure 22 and tables 1 and 2 suggest that the H2/S=3 family is globally always stiffer than the others. However, as written above, it is also always the heavier and should always be rejected, except for very small values of Ψ. According to the above comments concerning the volume, if only families S1, S2 and Q1 remain, one can conclude that, concerning the stiffness:

- For small and middle spans, the simplex S1/S2 with S=5 is very good (L/600 up to L/800);
- S1/S2 with S=4 or S=3 also offer a very good stiffness for growing values of Ψ;
- For large spans, the simplex S1 (or S2) with 3 or 4 modules offers the stiffest solutions;
- Family Q1 with S=4 or S=5 also offers competitive solutions, especially for high values of Ψ.

Finally, taking into account both the aspects of volume and stiffness, the simplex family has shown its superiority, followed by the Q1/S=4 or S=5 family.

8. Comparison between a tensegrity footbridge of topology S1/S2 and a truss footbridge

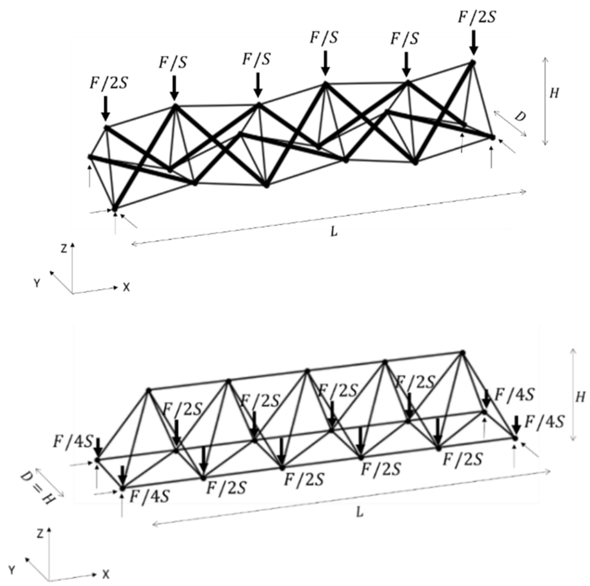

Fig. 23. Comparison between a “classical” truss composed of 5 pyramidal modules and a tensegrity structure of topology S1/S2 with S=5.

A tensegrity structure of topology S1,S2 (simplex with straight or sinusoidal deck), composed of 5 simplex modules, is here compared with a truss composed of 5 pyramidal modules (figure 23). The loads are uniformly distributed on the deck-level of the truss and steel is also used for each element (in such way that all elements in tension have the same cross section and all elements in compression have the same cross section). Figure 24 shows that, for a span of 40m, the tensegrity structure is always about 3 to 4 times heavier (83/27=3,1 and 18/4=4,5) than the lightest truss. This important result is largely discussed in the conclusion and must be nuanced. The truss is also slightly stiffer, and corresponds to lower values of L/H or, in other words, the tensegrity structure has to be slender than the truss to reach an optimum self-weight.

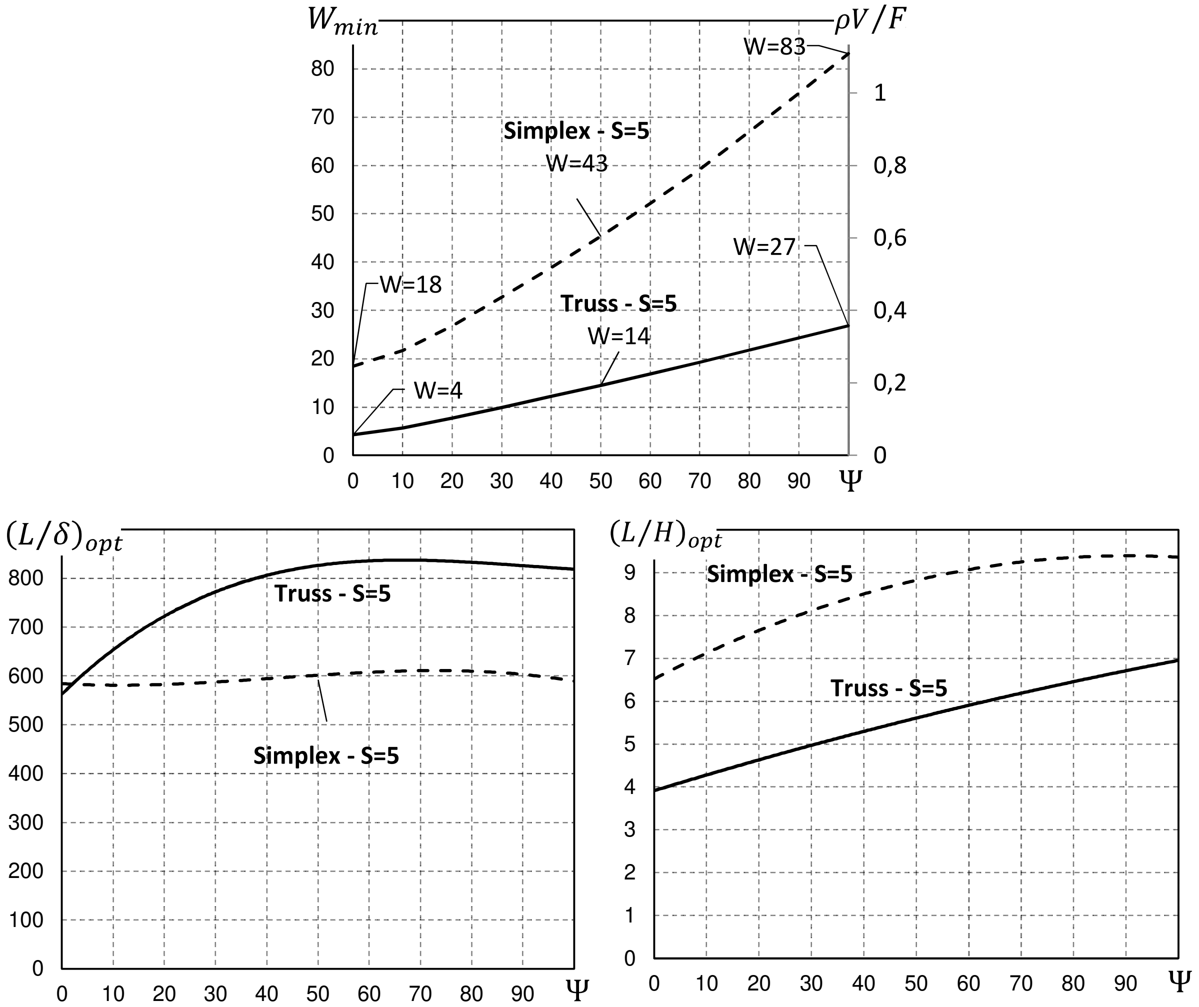

Fig. 24. Comparison between the efficiency curves of W for a truss with S=5 (in continuous line) and for a simplex topology with S1/S2-S=5 (in dashed line) for L=40m and Φ=125.10^{-4}, regardless any constraint related to the deck's width or the headroom.

9. Practical example: 40 m span tensegrity footbridge

The assumptions are the following:

- Span L=40m;
- Deck width b=2m;
- Struts: hollow circular cross sections with a ratio e/d=0.1, that means a factor q equal to 0.363 (figure 6);
- Cables: full cross sections;
- All materials in S355 steel (σ=237MPa, E=210.000 MPa, E/σ=886, ρ=77kN/m^3);

- Self-weight and other dead loads related to the deck are estimated at $1kN/m^2$ and live loads acting on the deck, included snow and wind, are estimated at $5,5kN/m^2$. This corresponds to a total load F= (1+5.5) *2*40=520kN.

The indicator of buckling is equal to $\Psi=\sigma_s L/(qE_sF)^{-1/2}$=48 and the indicator of self-weight is equal to $\Phi=\rho L/\sigma$=0.0125.

Figure 25 shows a few acceptable solutions, both in terms of volume and stiffness. The lightest solution corresponds to the structure made out of simplex S2 (snake deck) with S=4, W=46 and L/δ=572 (the corresponding point is illustrated in figure 22). The self-weight is about 7,8kN/m, which is not so unusual for footbridges. The example shows the benefit of the sinusoidal deck compared with the straight deck: 311kN instead of 372kN for the topology S1/S=4. Regarding the stiffness, the best structure is the H2/S=3, which reaches a value of L/786, but for a self-weight that grows up to 16,2 kN/m, i.e. the double of the S2/S=4 structure. The structure H1/S=3 is not really interesting since its volume is almost as high as the one of the H2/S=3, for a deflection similar to the S2/S=5 structure.

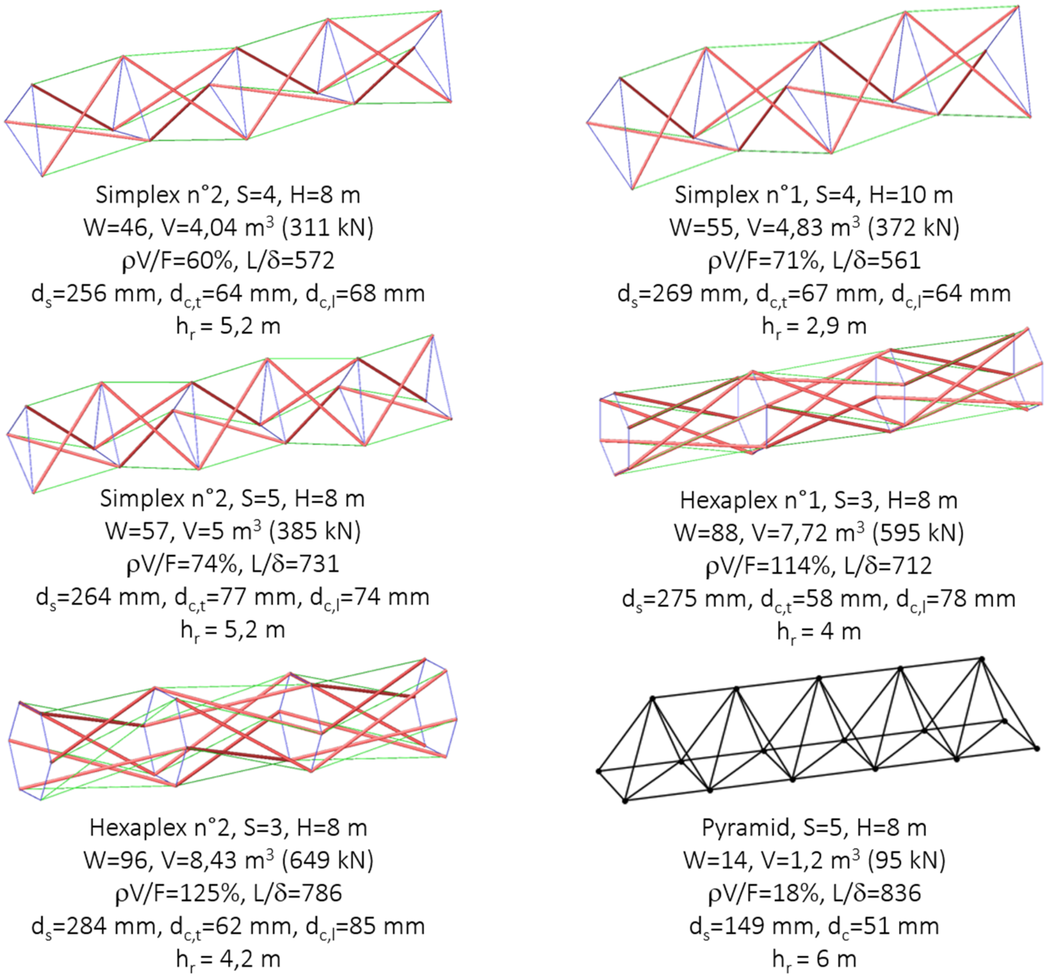

Fig. 25. The best solutions in terms of volume and/or deflection (b=2m).

Note however that:

- The structure composed of simplex S1 (straight deck) with S=4 offers a good solution with W=55, L/δ=561 and a headroom of 2.9m, mainly because it corresponds to the lightest structure with a straight deck;
- The structure composed of simplex S2 (snake deck) with S=5 also offers a good solution with W=57, L/δ=731 and a headroom of 5.2m;
- The last structure is a truss composed of 5 pyramidal modules as presented in the previous section. Its stiffness is globally slightly better than the one of the tensegrity structures

(L/δ=836). However, its self-weight is much lower with a W=14, to be compared with the best tensegrity having a W of 46. The lightest tensegrity structures are thus, here, more than 3 times heavier than the truss. This result is largely discussed in the conclusion and must be nuanced.

Finally, figure 26 shows the lightest structure with no restriction on the headroom and the deck width: here, imposing $b \geq 2$ increases of the mass of 11% (in comparison with the simplex S2/S=4 related to W=46).

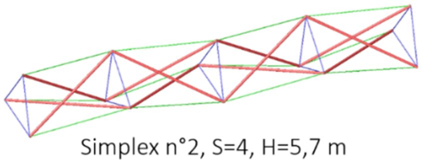

Fig. 26. The lightest tensegrity structure composed of prismatic modules.

The severity of the dynamic interaction with walking pedestrians is assessed by means of a modal analysis. Table 3 summarizes the natural frequencies computed for both the S2/S=4 tensegrity structure of figure 26 and the truss of figure 25. They are calculated with the tangent stiffness matrix of the structure, considering the self-weight load case and the lumped mass matrix. The first three torsional modes are much lower for the tensegrity structure (0.15Hz, 0.34Hz, 0.45Hz) than for the truss (32.0Hz, 59.5Hz, 99.7Hz), which confirms the greater deformability of the former system in torsion, as well as an increased mass compared to the truss. The fundamental bending mode in the vertical plane is above 30Hz, which confirms the very large stiffness of the tensegrity structure in the vertical direction. More importantly, the bending mode in the vertical direction and the torsional modes — which have a component in the vertical direction— are outside the main critical range corresponding to the vertical dynamic loading of walking pedestrians, i.e. [1.7Hz-2.1Hz]; quite far in fact. Furthermore, in the horizontal direction, only torsional modes —which have a component in the horizontal direction too— need to be considered. Their natural frequencies also lie outside the main critical range for resonance with human walk, i.e [0.5Hz-1.1Hz]. This is not the case for the truss structure which features a horizontal mode shape at 1.09Hz. This problem could be fixed by changing the support conditions of the truss but this goes beyond the scope of this paper. Finally, it is also noticed that the more important mass of the tensegrity structure makes it less prone to human-structure synchronization (Sétra, 2006) and vandalism excitation (Schwartz et al, 2014).

Simplex S2, S=4, H=5.7m		
Mode 1	0.15 Hz	First torsional vibration mode
Mode 2	0.34 Hz	Second torsional vibration mode
Mode 3	0.45 Hz	Third torsional vibration mode
Mode 4	30.2 Hz	First bending mode in vertical plane
Mode 5	55.9 Hz	First bending mode in horizontal plane
Truss S=5, H=8m		
Mode 1	1.09 Hz	Shear deformation in horizontal plane
Mode 2	26.0 Hz	First swaying mode
Mode 3	32.0 Hz	First torsional vibration mode
Mode 4	59.5 Hz	Second torsional vibration mode
Mode 5	99.7 Hz	Third torsional vibration mode

Table 3. Natural frequencies computed for both the tensegrity structure (simplex S2) and the truss.

10. Discussion and conclusion

As written in the abstract, the architectural potential of tensegrity structures is proven, yet, paradoxically, very few real construction projects have sprung up around the world. This fact has motivated the authors to prove the practical feasibility of such structures. This work needed a first important research summarized in (Latteur et al, 2017), which has offered the possibility of using a rigorous design and optimization methodology based on morphological indicators. Thanks to this design methodology, it has been possible to select the stiffest and the lightest footbridge structures, while also considering design constrains such as the headroom and the deck-width, in order to prove, or at the contrary to reject, the feasibility of some topologies. This article highlights the good performances of several topologies, in particular the simplex S1,S2, which often reaches a stiffness better than $L/600$ when subjected both to live loads and self-weight (that means excellent performances under live loads only).

The results presented in this article rely on several assumptions detailed in section "Assumptions and definitions". The practical case developed in the previous section shows that, even if the results in terms of stiffness and dynamic behavior are unexpectedly excellent for some topologies, the volume of such structures remains higher than the one related to more classical ones as trusses. However, the pyramidal truss is among the lightest structures for crossing a span. A comparison with other kinds of structures composed of bended beams or non-funicular arches (which is often an architect's choice) would certainly lead to much heavier structures than the truss, much more similar to tensegrity structures in terms of material consumption. For instance, considering again the example of previous section, but using this time 2 steel beams to cross the span and support the deck, a solution could be : two HL1000x554 steel profiles, with a stiffness of $L/476$ and a total self-weight equal to 444kN (deck not included), that means 11.1kN/m. This value has to be compared with the 7,8kN/m for the lightest tensegrity structure. Furthermore, the fundamental frequency of the beams would be equal to 2.1Hz, which is inside the critical range for pedestrians. This simple example proves that the tensegrity structure is not necessary a solution to avoid and not necessary too heavy when compared to other kinds of structures, or special architectural structures.

Furthermore, there exist several tracks for investigation in order to reduce the self-weight of tensegrity structures used as footbridges:

- Materials:
  The *efficiency curves of W* presented in this article are related to steel with $E_s/\sigma_s = E_c/\sigma_c = 886$ and $\sigma_s = \sigma_c = 237$MPa. However, for cables, other mechanical characteristics could be considered, for instance $\sigma_c = 1000$MPa and $E_c/\sigma_c = 210$, while struts are designed as before with $E_s/\sigma_s = 886$. Considering again the example of figure 26 (S=4 and L/H=40/5.7=7.0, redrawn in figure 27/0), figure 27/2 shows that decreasing ratio E_c/σ_c involves a lower self-weight (W=31), but also a lower stiffness (L/δ=175). It seems thus relevant to cleverly tune the materials properties (E,σ,ρ) in order to minimize the self-weight while ensuring sufficient stiffness. However, it remains uneasy to compare structures with different materials used for the struts as far as W itself depends on factors E_s/σ_s and on the indicator of buckling Ψ (according to equation (2b)). However, this limitation disappears if the structures have a linear behavior, as explained in the conclusion of (Latteur et al, 2017).
- Pre-stress level:
  This article assumes that the pre-stress level $\beta = \beta_{min}$ is fixed at its minimum, in such way that no cable slacks. Figure 27/3 shows that the stiffness can be improved (L/δ=1129) by increasing the pre-stress level or, in other words, by considering θ>1 (with $\beta = \theta\beta_{min}$). However, this has also a negative impact on the self-weight (W=69 for θ=2).

On the contrary, considering no pre-stress (θ=0) with cables replaced by struts designed according to (1b) leads to very low efficient structures in terms of both self-weight and stiffness, as shown in figure 27/1 (L/δ=297, W=59 for θ=0).

Finding an compromise between the material stiffness indicators E/σ and the pre-stress level β, both having an influence on the stiffness and the self-weight (figure 27/4), would thus be an interesting investigating path.

- Optimization of the pre-stress state:

  As explained in section ”External loads, self-weight, pre-stress and security coefficients”, one of the main assumptions of the design and optimization methodology relies on the choice of a pre-stress state, which may not lead to the optimum structures. In other words, researching a way to insert the optimization of the pre-stress state directly into the design methodology seems to be a relevant, and perhaps promising, research field.

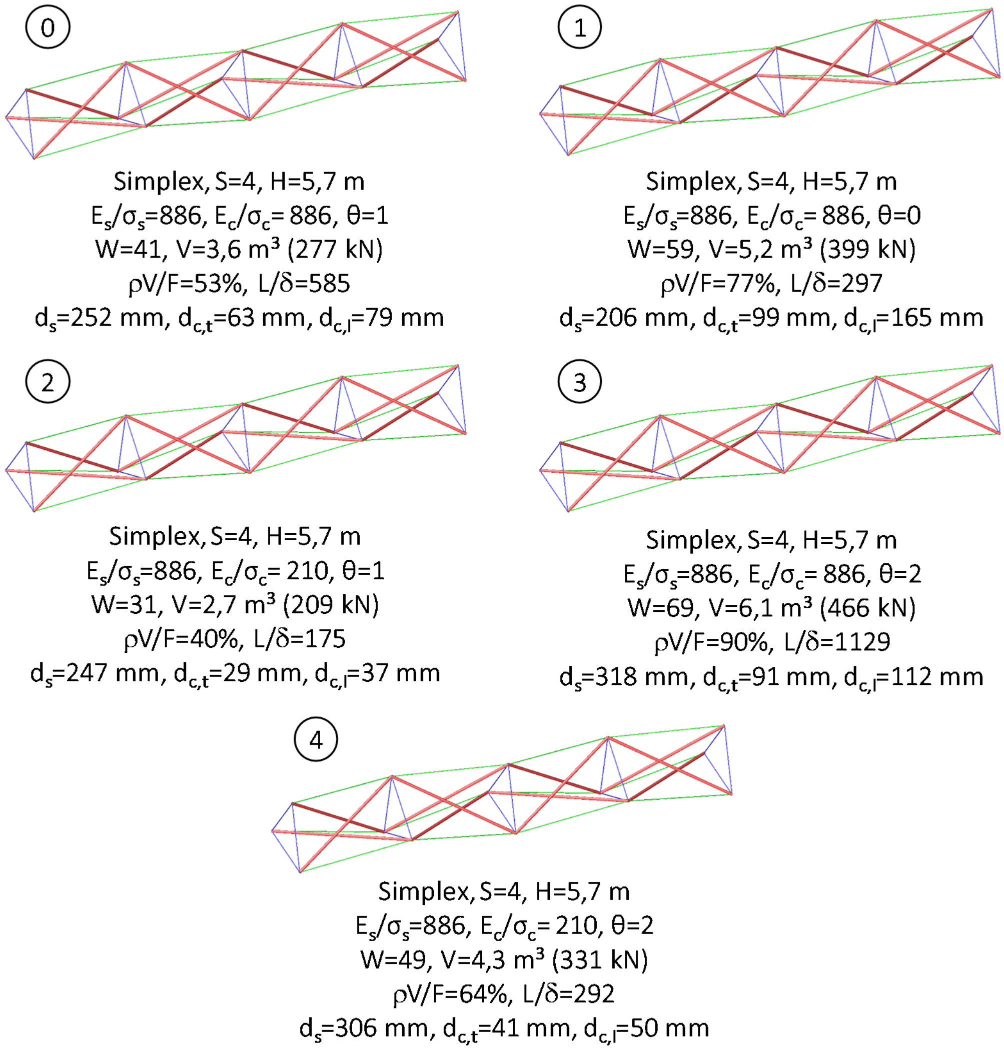

Fig. 27. Influence of the material stiffness indicator E/σ and the pre-stress level $\beta=\theta\beta_{min}$ on the stiffness L/δ and self-weight W of a structure (S an L/H are fixed).

Finally, other aspects linked to the robustness and to the practical construction should also be considered before any real construction.

Acknowledgements

Authors would like to thank BESIX Group SA for supporting this work.

Notation

The following symbols are used in this paper:

A : cross sectional area;
A_c , $A_{c,i}$: cross sectional area of a cable of index i;
$A_{c,l}$: cross sectional area of a longitudinal cable (horizontal direction);
$A_{c,t}$: cross sectional area of a transversal cable (triangular or polygonal bases);
A_s , $A_{s,i}$: cross sectional area of a strut of index i;
b : width of the suspended deck;
d : diameter of a cross section, or deflection under self-weight;
d_s : diameter of the cross section of a strut;
$d_{c,l}$: diameter of the cross section of a longitudinal cable;
$d_{c,t}$: diameter of the cross section of a transversal cable;
D : width of the structure before application of external load $\tilde{\mathbf{F}}$;
D_r : degree of redundancy of the structure;
e *:* steel thickness for a hollow section;
E : Young modulus;
E_c : Young modulus of the cables' material;
E_s : Young modulus of the struts' material;
F : see definition of $\tilde{\mathbf{F}}$;
$\tilde{\mathbf{F}}$ *:* vector defined in section "External loads, self-weight, pre-stress and security coefficients";
$\tilde{\mathbf{f}}$ *:* vector defined in section "External loads, self-weight, pre-stress and security coefficients" ;
F_{pre}, $F_{pre,i}$ *:* value of the "equivalent" pre-stress into a cable or a strut of index i, considered as an external axial load acting at both extremities of a cable (>0 because in traction) or a strut (<0 because in compression);
$\tilde{\mathbf{F}}_{\mathbf{pre}}$ *:* vector defined in section "External loads, self-weight, pre-stress and security coefficients";
$\tilde{\mathbf{f}}_{\mathbf{pre}}$: unit defined in section "External loads, self-weight, pre-stress and security coefficients";
f : undefined function;
$\tilde{\mathbf{G}}$ *:* self-weight of the structure, considered acting as an external load case in combination with the external load $\tilde{\mathbf{F}}$;
H : height of the structure;
h_r *:* available headroom for the pedestrians;
H1 : family of structures composed of hexaplex of type 1;
H2 : family of structures composed of hexaplex of type 2;
I_s, $I_{s,i}$: cross section moment of inertia of a strut of index i;
i,j,k : integers used for iterations (=0, 1, 2, …), or index of a node, of a strut or a cable;
k *:* maximum number of struts in contact with each other;
L : span of the structure;
L_0, $L_{0,i}$: length of a member (strut or cable) of index i when the structure is only subjected to the pre-stress $\tilde{\mathbf{P}}$;
m : equal to ratio e/d;
n : number of nodes;
n_c : number of cables;
n_s : number of struts;
$N_{c,i}$: axial force in a cable of index i, positive because always in traction, when the structure is subjected to the external load $\tilde{\mathbf{F}}$, prestress $\tilde{\mathbf{P}}$ and self-weight $\tilde{\mathbf{G}}$;

$N_{s,j}$: axial force in a strut of index j, negative because always in compression, when the structure is subjected to the external load $\tilde{\mathbf{F}}$, prestress $\tilde{\mathbf{P}}$ and self-weight $\tilde{\mathbf{G}}$;

P, P_i : value of the pre-stress into a cable (>0 because in traction) or a strut (<0 because in compression) of index i, before application of the external load

P1 : family of structures composed of pentaplex of type 1;

P2 : family of structures composed of pentaplex of type 2;

$\tilde{\mathbf{P}}$: vector defined in section "External loads, self-weight, pre-stress and security coefficients" ;

$\tilde{\mathbf{p}}$: vector defined in section "External loads, self-weight, pre-stress and security coefficients" ;

q : defined only for struts as $q = I_s / A_s^2$;

Q1 : family of structures composed of quadruplex of type 1;

Q2 : family of structures composed of quadruplex of type 2;

R_s : number of support reactions;

S : number of elementary tensegrity modules that compose the structure;

S1 : family of structures composed of simplex, with a straight deck;

S2 : family of structures composed of simplex, with a sinusoidal deck;

t_i^F : one value of vector $\tilde{\mathbf{f}}$;

t_i^P *: one value of vector* $\tilde{\mathbf{p}}$;

t_i^{pre} *: one value of vector* $\tilde{\mathbf{f}}_{\mathbf{pre}}$;

u : $=\sigma_c/\sigma_s$;

V : volume of materials (cables + struts);

W, W_{min} : indicator of volume, equal to $\sigma_s V/FL$;

Ψ : buckling indicator of the structure, equal to $\sigma_s L/(qE_sF)^{1/2}$;

β, β_{pre} : factor>0 defining the pre-stress level;

β_{min} ,$\beta_{pre,min}$: value of β or β_{pre} under which the least tensioned cable slacks when the loads are applied;

$\Phi_c = \rho_c L/\sigma_c$ and $\Phi_s = \rho_s L/\sigma_s$: indicators of self-weight related to cables and to struts;

Φ : value of the indicator of self-weight when $\Phi_c = \Phi_s$;

δ : deflection somewhere, for instance at mid span, due to live loads and self-weight acting together;

λ_i : slenderness of a strut of index i, equal to $L_{0,i}\sqrt{A_{s,i}/I_{s,i}}$;

Λ_i : equal to $\lambda_i \Big/ \left(\pi\sqrt{E_s/\sigma_s}\right)$;

υ : fundamental frequency in [Hz];

ρ : volumic weight of a material;

ρ_c : volumic weight of the material used for the cables;

ρ_s : volumic weight of the material used for the struts;

σ_c : maximum allowable stress in cables (including a security coefficient);

σ_s : maximum allowable stress in struts (including a security coefficient);

σ : can be σ_c or σ_s;

θ : real number ≥1 related to the pre-stress level.

References

Amouri S, Averseng J., Quirant J. and Dubé J-F. (2014). “Structural design and control of modular tensegrity structures”, European Journal of Environmental and Civil Engineering, Volume 19, Issue 6, pp 687-702.

Averseng J. and Dubé J.F. (2012). “Design, Analysis and Self Stress Setting of a Lightweight Deployable Tensegrity Modular Structure”, Procedia Engineering, Volume 40, Pages 14-19.

Bel Hadj Ali N., Rhode-Barbarigos L., Pascual Albi A. and F.C. Smith I. (2010). “Design optimization and dynamic analysis of a tensegrity-based footbridge”, Engineering Structures 32, 3650–3659.

Briseghella B., Fenu L., Huang W. and Zordan T. (2010). “Tensegrity Bridge with Prestressed Deck”, In IABSE Symposium Report Vol. 97, No. 22, pp. 71-78. [online] available at : https://www.researchgate.net/publication/233712079_Tensegrity_Bridge_with_Prestressed_Deck [Accessed 02 Sept. 2018].

Carpentieri G., Skelton R.E. and Fraternali F. (2015). “Minimum Mass and Optimal Complexity of Planar Tensegrity Bridges”, International Journal of Space Structures, Vol 30, Issue 3-4, pp. 221 – 243.

Davey P. and Forster K.W. (2007). “Exploring Boundaries: The Architecture of Wilkinson Eyre”, Walter de Gruyter, 114-115.7.

De Boeck J. (2013). “Tensegrity bridges: Concept design of pedestrian bridges using tensegrity as load carrying system”, Delft University of Technology. [online] available at : https://repository.tudelft.nl/islandora/object/uuid%3Abdab80b7-ed0e-4236-8e8f-74ff4ac75be5 [Accessed 02 Sept. 2018].

Eekhout M. (2016). “Lectures on innovation in building technology: Lecture articles for students of architecture”, Delft 1992-2015 / Nottingham 2005-2011, Amsterdam, The Netherlands, IOS Press BV, pp 167 – 178.

Eurocode NBN EN 1990/A1, Eurocode - Bases de calcul des structures - Annexe A2 : Applications aux ponts (+ AC:2008, AC:2010).

Grozdanic L. (2011). “Splash – A Building to Building Bridge formed by exploding glass / Joel Cullum – eVolo”, Architecture Magazine. Available at: http://www.evolo.us/architecture/splash-a-building-to-building-bridge-formed-by-exploding-glass-joel-cullum [Accessed 11 Mar. 2018].

Hanaor A. (2012). “Debunking Tensegrity - A Personal Perspective”, International Journal of Space Structures, Vol 27, Issue 2-3, pp. 179 – 183.

Heinemeyer C., Butz C., Keil A., Schlaich M., Goldack A., Lukic M., Chabrolin B., Lemaire A., Martin P., Cunha A., and Caetano E., (2009). Design of Lightweight Footbridges for Human Induced Vibrations - Background document in support to the implementation, harmonization and further development of the Eurocodes. JRC-ECCS 2009.

Jáuregui V.G. (2010). “Tensegrity structures and their application to architecture”, PUbliCan. [online] available at: https://www.researchgate.net/profile/Valentin_Gomez-Jauregui/publication/228781961_Tensegrity_structures_and_their_application_to_architecture/links/00b4952f5626eece30000000/Tensegrity-structures-and-their-application-to-architecture.pdf [Accessed 02 Sept. 2018].

Latteur P. (2000). Optimisation et prédimensionnement des treillis, arcs, poutres et câbles sur base d'indicateurs morphologiques. Application aux structures soumises en partie ou en totalité au flambement ». Thèse de doctorat, Vrije Universiteit Brussel.

Latteur P., Samyn P. and De Wilde P. (2000). "Comparaison des treillis classiques de type Warren, Pratt et Howe : optimisation et prédimensionnement sur base d'indicateurs morphologiques", Revue française de génie civil, Vol.4, no. 4/2000.

Latteur P., Samyn P. and De Wilde P. (2001). "Optimisation des arcs paraboliques et en chaînette – aide à la conception sur base d'indicateurs morphologiques", Revue française de génie civil, Vol.5, no. 1/2001.

Latteur P., Feron J. and Denoël V. (2017). “A design methodology for lattice and tensegrity structures based on a stiffness and volume optimization algorithm using morphological indicators”, IASS, Volume 32, issue: 3-4, p. 226-243.

Micheletti A., Nicotra V., Podio-Guidugli P. and Stucchi S. (2005). “The tensegrity footbridge at Torvergata University in Rome”, In Proc. of the 2nd international conference footbridge (pp. 159-160).

Micheletti A. (2012). “Modular Tensegrity Structures: The ”Tor Vergata” Footbridge”, Mechanics, Models and Methods in Civil Engineering, vol 61, pp 375-384.

Michell A.G.M. (1904). “The limit of Economy of Material in Frame Structures”. Philosophical Magazine, S.6, Vol. 8, n° 47, p. 589-597.

Motro R. (2005). « Tenségrité », Hermes Science, Paris.

Motro R., Maurin B and., Silvestri C. (2006). “Tensegrity rings and the hollow rope”, In: IASS symposium 2006, new olympics, new shells and spatial structures. Beijing, p. 470-1.

Mucedola M. and Paradiso S. (2013). “Suspended Tensegrity Bridge”, [online] Issue. Available at: https://issuu.com/stefanoparadiso3/docs/tesi_mucedola_paradiso [Accessed 23 Mar. 2018].

Rhode-Barbarigos L., Bel Hadj Ali N., Motro R. and F.C. Smith I. (2010). “Designing tensegrity modules for pedestrian bridges”, Engineering Structures 32, 1158–1167.

Rhode-Barbarigos L., Jain H., Kripakaran P. et al. (2010). “Design of tensegrity structures using parametric analysis and stochastic search”, Engineering with Computers Vol 26, Issue 2, 193-203.

Rhode-Barbarigos L., Bel Hadj Ali N., Motro R. and F.C. Smith I. (2012). “Design aspects of a deployable tensegrity-hollow-rope footbridge”, International Journal of Space Structures, 27(2), 81-96.

Rolvink A., van de Straat R. and Coenders J. (2010). “Parametric Structural Design and beyond”, International Journal of Architectural Computing, Vol 8, Issue 3, pp. 319 – 336.

Schwartz, C., Berger, A., Bruls, O., Forthomme, B., Croisier, J.-L., & Denoël, V. (2014). Experimental Study of the Human Ability to Deliberately Excite a Flexible Floor. In A., Zingoni (Ed.), Proceedings of the 5th International Conference on Structural Engineering, Mechanics and Computation.

Sétra/AFGC, (2006). Evaluation du comportement vibratoire des passerelles piétonnes sous l’action des piétons (Assessment of vibrational behavior of footbridges under pedestrian loading), Association Française de Génie Civil.

Skelton R. E. and de Oliveira M. (2009). “Tensegrity systems”, Springer Science+Business Media, p. 1-7.

Skelton R.E., Fraternali F., Carpentieri G. and Micheletti A. (2014). “Minimum mass design of tensegrity bridges with parametric architecture and multiscale complexity”, Mechanics Research Communications, Volume 58, Pages 124-132, ISSN 0093-6413.

Sychterz C. and F.C. Smith I. (2017). “Joint Friction during Deployment of a Near-Full-Scale Tensegrity Footbridge”, Journal Of Structural Engineering, vol. 143, num. 9, p. 04017081.

Van den Broeck P. and De Roeck G., (2012). Tricon: Prediction and control of human-induced vibrations of civil engineering structures. financed by the Flemish government: IWT, agency for Innovation by Science and Technology.

Veuve N., Safaei S. D. and F. C. Smith I. (2015). “Deployment of a tensegrity footbridge”, Journal of Structural Engineering, vol. 141, num. 11, p. 211-218.

WilkinsonEyre, [online] available at: http://www.wilkinsoneyre.com/projects/tensegrity-bridge [Accessed 02 Sept. 2018].